

Modeling the *Trichodesmium* sp. related N₂ fixation : driving processes and impacts on primary production in the tropical Pacific Ocean

Dutheil Cyril^{1,2}, Aumont Olivier², Gorguès Thomas³, Lorrain Anne⁴, Bonnet Sophie⁵, Rodier Martine⁶, Dupouy Cécile^{1,5}, Shiozaki Takuhei⁷, and Menkes Christophe^{1,2}

¹Centre IRD, Nouméa, New Caledonia

²LOCEAN Laboratory, IPSL, Sorbonne Universités (UPMC, Univ Paris 06)-CNRS-IRD-MNHN, Paris, France

³Laboratoire d'Océanographie Physique et Spatiale (LOPS), Univ. Brest-CNRS-Ifremer-IRD, Plouzané, France

⁴LEMAR, UMR 6539, UBO-CNRS-Ifremer-IRD, IUEM, Plouzané, France

⁵Aix Marseille Université, CNRS/INSU, Université de Toulon, IRD, Mediterranean Institute of Oceanography (MIO) UM 110, 13288, Marseille, France

⁶Environnement Insulaire Océanien (EIO), UMR 241(Univ. de Polynésie Française, IRD, ILM, IFREMER), Tahiti, French Polynesia

⁷Research and Development Center for Global Change, Japan Agency for Marine-Earth Science and Technology, Yokosuka, Japan

Correspondence: Cyril Dutheil (cyril.dutheil@ird.fr)

1 **Abstract.** Dinitrogen fixation is now recognized as one of the major sources of bio-available nitrogen in the ocean. Thus,
2 N₂ fixation sustains a significant part of the global primary production by supplying the most common limiting nutrient for
3 phytoplankton growth. The «Oligotrophy to UItra-oligotrophy PACific Experiment» (OUTPACE) improved the data coverage
4 of the Western Tropical South Pacific, an area recently recognized as a hotspot of N₂ fixation. This new development leads
5 us to develop and test an explicit N₂ fixation formulation based on the *Trichodesmium* physiology (the most studied nitrogen
6 fixer) within a 3D coupled dynamical-biogeochemical model (ROMS-PISCES). We performed a climatological numerical
7 simulation that is able to reproduce the main physical (e.g Sea Surface Temperature) and biogeochemical patterns (nutrients,
8 and chlorophyll concentrations as well as N₂ fixation) in the tropical Pacific. This simulation displayed a *Trichodesmium*
9 regional distribution that extends from 150°E to 120°W in the south tropical Pacific, and from 120°E to 140°W in the north
10 tropical Pacific. The local simulated maximums were found around islands (Hawaii, Fiji, Samoa, New Caledonia, Vanuatu).
11 We assessed that 15% of the total primary production may be due to *Trichodesmium* in the Low Nutrient, Low Chlorophyll
12 regions (LNLC) of the Tropical Pacific. Comparison between our explicit and the often used (in biogeochemical models)
13 implicit parameterization of N₂ fixation showed that the latter leads to an underestimation of N₂ fixation rates by about 25% in
14 LNLC regions. Finally, we established that iron fluxes from island sediments control the spatial distribution of *Trichodesmium*
15 biomasses in the western tropical south Pacific. Noteworthy, this last result does not take into account the iron supply from
16 rivers and hydrothermal sources, which may well be of importance in a region known for its strong precipitation rates and
17 volcanic activity.

18 1 Introduction

19 Nitrogen is known to be the most common limiting nutrient for phytoplankton growth in the modern world ocean (Moore et al.,
20 2013), especially in the Low Nutrient, Low Chlorophyll (LNL) ecosystems (Arrigo, 2005; Gruber, 2005). Characterizing the
21 processes governing nitrogen sources and sinks to and from the ocean is therefore central to understanding oceanic production,
22 organic matter export and food web structure. Atmospheric dinitrogen (N_2) dissolved in seawater is by far the dominant form
23 of N present in the ocean, i.e. the $N_2:NO_3^-$ ratio typically exceeds 100 in surface waters. However, most phytoplankton species
24 cannot assimilate N_2 , and grow using reactive forms of nitrogen such as nitrate, ammonium and dissolved organic compounds.
25 Some planktonic prokaryotic microorganisms, called “diazotrophs” use an enzyme, the nitrogenase, to fix N_2 and convert it
26 into ammonia (NH_3) and ultimately ammonium (NH_4^+). At the global scale, they provide the major external source of reactive
27 nitrogen to the ocean (Gruber, 2008), and support up to 50% of new production in tropical and subtropical (LNL) regions
28 (Bonnet et al., 2009; Capone, 1997; Deutsch et al., 2007b; Karl et al., 1997; Moutin et al., 2008; Raimbault and Garcia,
29 2008). These organisms are physiologically and taxonomically diverse including cyanobacteria, bacteria and archaea (Zehr
30 and Bombar, 2015; Delmont et al., 2017).

31 Autotrophic diazotrophs have been far more intensively studied than heterotrophic diazotrophs, whose contribution to global
32 N_2 fixation remains unclear (Turk-Kubo et al., 2014; Bombar et al., 2016; Moisander et al., 2017). Autotrophic diazotrophs
33 have been characterized both in the field and through laboratory experiments and their physiology is consequently better
34 known (Bergman et al., 2013; Küpper et al., 2008; Mulholland and Capone, 2001, 2000; Ohki et al., 1992; Ramamurthy and
35 Krishnamurthy, 1967; Rubin et al., 2011). Cyanobacterial (autotrophic) diazotrophs are composed of 3 main groups: 1) the
36 filamentous diazotrophs including the colonial, non-heterocyst-forming *Trichodesmium*, 2) the heterocyst-forming symbionts
37 associated with diatoms (DDAs), and 3) the unicellular cyanobacterial diazotrophs (UCYN, phylogenetically divided into three
38 groups : UCYN-A, B, and C). It has been established that autotrophic diazotrophs growth rates are typically one order of
39 magnitude lower than those of non-diazotrophs (Breitbarth et al., 2008; Falcón et al., 2005; Goebel et al., 2008; LaRoche
40 and Breitbarth, 2005). This can be related to the high energetic demand (Postgate, 1982) required to convert N_2 to NH_3 as
41 compared to that necessary to assimilate nitrate or ammonia. This low growth rate (compared to other phytoplankton species)
42 mainly constrains their ecological niches to nitrate-poor regions, where they can be competitive. Moreover, their geographical
43 distribution is constrained by nutrient availability in the photic layer (mainly iron and phosphate) (Berman-Frank, 2001; Bonnet
44 et al., 2009; Mills et al., 2004; Moutin et al., 2005, 2008; Rubin et al., 2011; Rueter, 1988) and temperature (Staal et al., 2003).
45 *Trichodesmium* sp. are present only in water where temperature is above 20°C (Capone, 1997; LaRoche and Breitbarth, 2005;
46 Montoya et al., 2004), while some UCYN can be found in colder and deeper waters (Bonnet et al., 2015; Church et al., 2005;
47 Moisander et al., 2010).

48 The spatial distribution and rates of N_2 fixation have been inferred at the global scale using several tools. Deutsch et al. (2007a)
49 have introduced the tracer P^* which represents the excess of P relative to the standard N quota. A decrease in this tracer is then
50 interpreted as N_2 fixation, since N_2 fixation extracts PO_4 alone. More recently, Luo et al. (2014) developed a multiple linear
51 regression that relates N_2 fixation from the MAREDAT database (Luo et al., 2012) to environmental conditions (nutrients, SST,

52 irradiance, MLD,...) in order to build a statistical model for global N₂ fixation distribution.
53 Numerical models have also been used as they allow to overcome the scarcity of observations that may limit the implementation
54 of the two previous approaches (Aumont et al., 2015; Bissett et al., 1999; Dutkiewicz et al., 2012; Keith Moore et al., 2006;
55 Krishnamurthy et al., 2009; Monteiro et al., 2011; Moore et al., 2013; Tagliabue et al., 2008). They can notably be used to
56 investigate the spatial and temporal variability of dinitrogen fixation and to study its controlling environmental factors. In these
57 models, N₂ fixation has been implemented in various ways. Some models use implicit parameterizations (Bissett et al., 1999;
58 Maier-Reimer et al., 2005; Assmann et al., 2009; Aumont et al., 2015) to derive N₂ fixation from environmental conditions
59 (mainly nitrate, phosphate and iron concentrations, temperature and light) without explicitly simulating any nitrogen fixing
60 organisms. Alternatively, other models rely on the explicit descriptions of diazotrophs (Moore et al., 2004; Dunne et al., 2013)
61 that have mainly been developed from the knowledge derived from laboratory experiments focused on *Trichodesmium* sp.
62 (Fennel et al., 2001; Hood et al., 2001; Moore et al., 2001). Noticeably, several modeling studies have been especially focused
63 on the role of iron in controlling the distribution of diazotrophs and N₂ fixation (Keith Moore et al., 2006; Krishnamurthy
64 et al., 2009; Moore et al., 2004; Tagliabue et al., 2008). Indeed, a realistic representation of marine iron concentrations has
65 been stressed as a key factor to adequately simulate the habitat of diazotrophs (Monteiro et al., 2011; Dutkiewicz et al., 2012).
66 Moreover, among the full set of studies focusing on the spatial distribution of N₂ fixation, some studies (Berthelot et al., 2017;
67 Bonnet et al., 2009, 2015; Garcia et al., 2007; Shiozaki et al., 2014) based on oceanographic campaigns have reported high
68 N₂ fixation rates in the Western Tropical South Pacific (WTSP), that has been recently identified as a globally important hot
69 spot of N₂ fixation with rates > 600 μmol N m⁻².d⁻¹ (Bonnet et al., 2017). Very high abundances of *Trichodesmium* have
70 been historically reported in this region (Dupouy et al., 2000, 2011; Moisaner et al., 2008; Neveux et al., 2006; Shiozaki
71 et al., 2014) Stenegren et al., This issue) and have recently been identified as the major contributor to N₂ fixation in this region
72 (Berthelot et al., 2017) Bonnet et al., This issue). However, the reasons for such an ecological success of diazotrophs in this
73 region are still poorly understood.

74 In this study, we aim at bringing new insights on this known, but poorly understood, “N₂ fixation hotspot”. This study ambitions
75 to understand the spatial and temporal distribution (i.e. seasonal variability) of *Trichodesmium* and to evaluate the potential
76 impact of *Trichodesmium* fixers on the biogeochemical conditions of the WTSP. We will specifically address the following
77 overarching questions: (i) What are the mechanisms that structure the *Trichodesmium* distribution in the WTSP, particularly
78 around the South West Pacific islands, and (ii) what is the biogeochemical impact of N₂ fixation in this region? Noteworthy,
79 this study is also taking advantage of the sampling done during the « Oligotrophy to UTRa-oligotrophy PACific Experiment »
80 (OUTPACE), which nicely complement the data coverage in the south west Pacific, and allow a better characterization of the
81 processes responsible for the spatial and seasonal variability of the N₂ fixation.

82 To fulfill our objectives, we have implemented an explicit representation of the nitrogen fixers, based on the *Trichodesmium*
83 physiology, in a biogeochemical model. The first section of this study describes the experimental design and the observations
84 used in our study, while the second part of the paper provides a validation of our reference simulation with an analysis of the
85 *Trichodesmium* compartment and its impacts on the biogeochemical conditions of the Tropical Pacific. In the discussion, the
86 impact of iron from islands sediment on dinitrogen fixation is considered as well as the added value of an explicit dinitrogen

87 fixer compartment rather than a simpler implicit representation of N₂ fixation. Finally, implications for and limits of our
88 modeling exercise are detailed in the conclusion.

89 **2 Methods**

90 **2.1 Coupled dynamical (ROMS)-biogeochemical (PISCES) model**

91 **2.1.1 ROMS**

92 In this study, we used a coupled dynamical-biogeochemical framework based on the regional ocean dynamical model ROMS
93 (Regional Oceanic Modeling System, (Shchepetkin and McWilliams, 2005) and a new version of biogeochemical model
94 PISCES (Pelagic Interactions Scheme for Carbon and Ecosystem Studies). The ocean model configuration is based on the
95 ROMS-AGRIF (Penven et al., 2006) computer code and covers the tropical Pacific region [33°S-33°N;110°E-90°W]. It has 41
96 terrain-following vertical levels with 2-5 m vertical resolution in the top 50 meters of the water column, then 10-20 m resolution
97 in the thermocline and 200-1000 m resolution in the deep ocean. The horizontal resolution is 1°. The turbulent vertical mixing
98 parameterization is based on the non-local K profile parameterization (KPP) of Large et al. (1994). Open boundaries condi-
99 tions are treated using a mixed active/passive scheme (Marchesiello et al., 2001). This scheme is used to force our regional
100 configuration with monthly climatological large-scale boundary conditions from a ½° ORCA global ocean simulation (details
101 available in Kessler and Gourdeau (2007)), while allowing anomalies to radiate out of the domain. The use of similar ROMS
102 configurations (e.g vertical resolution, mixed active/passive scheme, turbulent vertical mixing parameterization) in the WTSP
103 is largely validated through studies demonstrating skills in simulating both the surface (Jullien et al., 2012, 2014; Marchesiello
104 et al., 2010) and subsurface ocean circulation (Couvelard et al., 2008).

105 To compute the momentum and fresh water/heat fluxes, we also use a climatological forcing strategy. Indeed, documenting
106 the inter-annual to decadal variability is beyond the scopes of our study, which justifies using climatological forcing fields.
107 A monthly climatology of the momentum forcing is computed from the 1993-2013 period of the ERS1-2 scatterometer stress
108 (<http://cersat.ifremer.fr/oceanography-from-space/our-domains-of-research/air-sea-interaction/ers-ami-wind>). Indeed, ERS de-
109 rived forcing has been shown to produce adequate simulations of the Pacific Ocean dynamics (e.g. Cravatte et al., 2007). A
110 monthly climatology at 1/2° resolution computed from the Comprehensive Ocean–Atmosphere Data Set (COADS; Da Silva
111 et al. (1994)) is used for heat and fresh water forcing. In our set-up, ROMS also forces on line a biogeochemical model using a
112 WENO5 advection scheme (i.e. five order weighted essentially non-oscillatory scheme; Shchepetkin and McWilliams, 1998).
113 After a one year spin-up we stored 1-day averaged outputs for analysis.

114 **2.1.2 PISCES**

115 In this study, we use a quota version of the standard PISCES model (Aumont and Bopp, 2006; Aumont et al., 2015), which
116 simulates the marine biological productivity and the biogeochemical cycles of carbon and the main nutrients (P, N, Si, Fe).
117 This modified model, called PISCES-QUOTA, is extensively described in Kwiatkowski et al. (2018). Our version is essentially

118 identical to Kwiatkowski's version that included an added picophytoplankton group, except that this latter group has been
 119 removed and replaced by a *Trichodesmium* compartment. Here we only highlight the main characteristics of the model and
 120 the specifics of our model version. Our version of PISCES-QUOTA has then 39 prognostic compartments. As in the standard
 121 PISCES version, phytoplankton growth is limited by the availability in five nutrients: nitrate and ammonium, phosphate, sil-
 122 icate and iron. Five living compartments are represented: three phytoplankton groups corresponding to nanophytoplankton,
 123 diatoms, and *Trichodesmium* and two zooplankton size-classes that are microzooplankton and mesozooplankton. The elemen-
 124 tal composition of phytoplankton and non-living organic matter is variable and is prognostically predicted by the model. On
 125 the other hand, zooplankton are assumed to be strictly homeostatic, i.e. their stoichiometry is kept constant (e.g. Meunier et al.,
 126 2014; Sterner and Elser, 2002). Nutrients uptake and assimilation as well as limitation of growth rate are modeled according to
 127 the chain model of Pahlow and Oschlies (2009). The P quota limits N assimilation which in turns limits phytoplankton growth.
 128 The phosphorus to nitrogen ratios of phytoplankton are described based on the potential allocation between P-rich biosynthesis
 129 machinery, N-rich light harvesting apparatus, a nutrient uptake component, the carbon stores, and the remainder (Daines et al.,
 130 2014; Klausmeier et al., 2004). This allocation depends on the cell size and on the environmental conditions.
 131 Nutrients are delivered to the ocean through dust deposition, river runoff and mobilization from the sediment. The atmospheric
 132 deposition of iron is derived from a climatological dust simulation (Tegen and Fung, 1995). The iron from sediment is recog-
 133 nized as a significant source (Johnson et al., 1999; Moore et al., 2004). This iron source is indeed parameterized in PISCES as,
 134 basically, a time-constant flux of dissolved iron ($2 \mu\text{mol.m}^{-2}.\text{day}^{-1}$) applied over the whole sediment surface and modulated
 135 depending only on depth. A detailed description of this sedimentary source is presented in Aumont et al. (2015). The initial
 136 conditions and biogeochemical fluxes (iron, phosphorus, nitrate, ...) at the boundaries of our domain are extracted from the
 137 World Ocean Atlas 2009 (<https://www.nodc.noaa.gov/OC5/WOA09/woa09data.html>).

138 2.1.3 *Trichodesmium* compartment

139 For the purpose of this study, we implemented in the PISCES-QUOTA version an explicit representation of *Trichodesmium*.
 140 Therefore, as already stated, five living compartments are modeled with three phytoplankton groups (nanophytoplankton,
 141 diatoms, and *Trichodesmium*) and two zooplankton groups (microzooplankton, and mesozooplankton). Similarly to nanophy-
 142 toplankton, the equation of *Trichodesmium* evolution is computed as follows:

$$\begin{aligned}
 \frac{\partial Tri_C}{\partial t} = & (1 - \delta^{Tri})\mu^{Tri}Tri - \zeta_{NO_3}^{Tri}V_{NO_3}^{Tri} - \zeta_{NH_4}^{Tri}V_{NH_4}^{Tri} - m^{Tri}\frac{Tri_C}{K_m + Tri_C}Tri_C \\
 & - sh \times \omega^{Tri}P^2 - g^Z(Tri)Z - g^M(Tri)M
 \end{aligned}
 \tag{1}$$

144 In this equation, Tri_C is the carbon *Trichodesmium* biomass, and the seven terms on the right-hand side represent respectively
 145 growth, biosynthesis costs based on nitrate and ammonium, mortality, aggregation and grazing by micro- and mesozooplankton.
 146 In our configuration, the photosynthesis growth rate of *Trichodesmium* is limited by light, temperature, phosphorus and iron
 147 availability. Photosynthesis growth rate of *Trichodesmium* μ^{Tri} is computed as follows:

$$\mu^{Tri} = \mu_{FixN_2}^{Tri} + \mu_{NO_3}^{Tri} + \mu_{NH_4}^{Tri}
 \tag{2}$$

149 where μ_{FixN_2} denotes growth due to dinitrogen fixation, $\mu_{NO_3}^{Tri}$ and $\mu_{NH_4}^{Tri}$ represent growth sustained by NO_3^- and NH_4^+ up-
150 take, respectively. Moreover, a fraction of fixed nitrogen is released back to seawater, mainly as ammonia and dissolved organic
151 nitrogen, by the simulated *Trichodesmium* compartment. Berthelot et al. (2015a) estimated this fraction to be less than 10%
152 when considering all diazotrophs. We set up this fraction at 5% of the total amount of fixed nitrogen. For the other nutrients
153 (i.e. iron and phosphorus), the same fraction is also released.

154 Dinitrogen fixation is limited by the availability of phosphate, iron and light and is modulated by temperature. Loss processes
155 are natural mortality, and grazing by zooplankton. Natural mortality is considered to be similar to the other modeled phyto-
156 plankton species. Grazing on *Trichodesmium* is rarely described, but it is admitted that *Trichodesmium* represents a poor source
157 of food for zooplankton (O'Neil and Romane, 1992) especially because they contain toxins (Hawser et al., 1992). On the other
158 hand, many species of copepods have been shown to be able to graze on *Trichodesmium* despite the strong concentrations
159 of toxins (O'Neil and Romane, 1992). For these reasons we applied two different coefficients for the grazing preference by
160 mesozooplankton and microzooplankton (Table 1). For microzooplankton, grazing preference is halved to account for *Tri-*
161 *chodesmium* toxicity, and for mesozooplankton the grazing preference is similar to that of the other phytoplankton species.
162 The complete set of equations of *Trichodesmium* is detailed in Appendix 1. Table 1 presents the parameters that differ between
163 Nanophytoplankton and *Trichodesmium*.

164 This setup reproduces dinitrogen fixation through an explicit representation of the *Trichodesmium* biomass (to be compared
165 with often used implicit parameterizations (Assmann et al., 2009; Aumont et al., 2015; Dunne et al., 2013; Maier-Reimer
166 et al., 2005; Zahariev et al., 2008) that links directly environmental parameters to nitrogen fixation without requiring the *Tri-*
167 *chodesmium* biomass to be simulated).

168 **2.2 Experimental setup**

169 Below are summarized the set of experiments that have been performed in this study (Table 2). All climatological simulations
170 have been run for 20-years from the same restart and only the last 19-years are considered in our diagnostics. We chose the
171 above described simulation explicitly modelling the *Trichodesmium* to be our reference experiment (hereafter referred to as
172 «TRI»). In a second experiment called «TRI_NoFeSed», the model setup is identical to the reference experiment, except that
173 iron input from the sediments is turned off between 156°E and 120°W. In a third experiment «TRI_imp», the explicit dinitrogen
174 fixation module is replaced by the implicit parameterization described in Aumont et al. (2015) where fixation depends directly
175 on water temperature, nitrogen, phosphorus and iron concentrations and light (no nitrogen fixers are simulated). Finally, a
176 fourth experiment «N2_Wo» corresponds to a model setup in which no explicit nor implicit description of dinitrogen fixation
177 is activated.

178 Comparison between TRI and TRI_NoFeSed experiments enables to estimate the impact of iron input from island sediments
179 on the dinitrogen fixation, while the impact of dinitrogen fixation on the biogeochemical conditions in the Pacific Ocean can
180 be investigated by comparing TRI and N2_Wo. Finally, the TRI and TRI_imp experiments are used to evaluate the added value
181 of an explicit description of dinitrogen fixation relative to an implicit inexpensive parameterization.

182 2.3 Observational datasets

183 Several different databases have been used to evaluate the model skills. For nitrate and phosphate, the CSIRO 1/2° global Atlas
184 of Regional Seas (CARS, <http://www.marine.csiro.au/dunn/cars2009/>) has been used. Iron has been evaluated with the global
185 database from Tagliabue et al. (2012) complemented with the dissolved iron data from the OUTPACE cruise (Guieu et al., un-
186 der review). This database is a compilation of 13125 dissolved iron observations covering the global ocean and encompassing
187 the period 1978–2008. The global MARine Ecosystem DATA (MAREDAT, <https://doi.pangaea.de/10.1594/PANGAEA.793246>)
188 database of N₂ fixation has been expanded with data from recent cruises performed in the WTSP: MOORSPICE (Berth-
189 elot et al., 2017), DIAPALIS (Garcia et al., 2007), NECTALIS ([http://www.spc.int/oceanfish/en/ofpsection/ema/biological-](http://www.spc.int/oceanfish/en/ofpsection/ema/biological-research/nectalis)
190 [research/nectalis](http://www.spc.int/oceanfish/en/ofpsection/ema/biological-research/nectalis)), PANDORA (Bonnet et al., 2015), OUTPACE (Bonnet et al., This issue), Mirai (Shiozaki et al., 2014). This
191 database contains 3079 data points at the global ocean scale, of which 1300 are located in our simulated region (Luo et al.,
192 2012). Finally, we have used surface chlorophyll concentrations from the GLOBCOLOUR project (<http://ftp.acri.fr>) which
193 spans the 1998-2013 time period.

194 3 Results

195 3.1 Model Validation

196 In this subsection, we aim at validating our reference simulation «TRI» with the data previously presented. In the Pacific,
197 phosphate and nitrate concentrations show maxima in the upwelling regions, i.e. along the western American coast, and in
198 the equatorial upwelling (Fig. 1a,c), and minima in the subtropical gyres. First, phosphate patterns show modeled values and
199 structures in qualitatively good agreement with observations, despite an underestimation in the areas of high concentrations as
200 within the Costa Rica dome and along the equator. In contrast, the nitrate structure shows larger biases. We observe concen-
201 trations higher than 1 $\mu\text{mol.L}^{-1}$ all along the equator in CARS, while in the model nitrate concentrations are lower than this
202 value west of 170W°. More generally the model tends to underestimate nitrate concentrations.

203 The regions most favorable for *Trichodesmium* can be defined by temperature within 25-29°C (Breitbarth et al., 2007). The
204 model reproduces relatively well the spatial distribution of this temperature preferendum. This distribution exhibits a significant
205 seasonal variability, mainly as a result of the variability of the 25°C isotherm. The latter moves by 7° latitudinally between
206 summer and winter in the WTSP, and by 15° in the Western Tropical North Pacific (WTNP) (Fig. 1a). This displacement
207 is well reproduced in the TRI simulation (Fig. 1b). By contrast, along the equator the mean position of the 25°C isotherm is
208 shifted eastward in the TRI simulation (120°W) compared to the observations (125°W; Fig. 1a vs 1b), but its seasonal dis-
209 placements are well reproduced except in the South-Eastern Pacific. Overall, this temporal variability is well reproduced by
210 the model (Fig. 1b), despite this bias. In contrast, nitrate and phosphate seasonal variability remains low (not shown).

211 Another important feature that needs to be properly reproduced by the model is the iron distribution in the upper ocean. We
212 have sampled the modeled values at the same time and same location as the data. The median value as well as the disper-
213 sion of the iron surface concentrations over the tropical Pacific, are displayed for both the data and the model in Figure 2a.

214 Mann-Whitney test reveals that these two normalized distributions are not significantly different (p-value = 0.26). Figures 2b,c
215 display respectively the observed iron field and the modeled values. The best sampled area is the central Pacific ocean where
216 simulated iron concentrations are low (0.1 to 0.3 nmol Fe.L⁻¹, Fig. 2c), which is consistent with the observations (Fig. 2b).
217 The southwest Pacific is characterized by relatively high surface iron concentrations, between 0.4 and 0.8 nmol Fe.L⁻¹, both
218 in the data and in the model. Large scale patterns are thus well represented by the model. Nevertheless, the model tends to
219 overestimate iron levels in the South Pacific gyre, between 180° and 140°W at about 20°S.

220 Figure 3 displays a comparison between surface Chlorophyll concentrations from GLOBCOLOUR data (a), and from TRI
221 (b) and TRI_imp (c) simulations. High chlorophyll concentrations are found in the eastern equatorial Pacific upwelling and
222 along Peru in both the observations and our two simulations, with mean values higher than 0.3 mg Chl.m⁻³. The equatorial
223 chlorophyll maximum simulated by the model (Fig. 3b,c) is however too narrow compared to the observations, especially in
224 the northern hemisphere. Similarly, the model is unable to simulate the elevated chlorophyll levels around the Costa Rica dome
225 and the localized enhanced chlorophyll off Papua New Guinea. In TRI (Fig. 3b), chlorophyll values in the South West Pacific
226 region vary between 0.1 and 0.2 mg Chl.m⁻³, with maxima located in the vicinity of the Fiji and Vanuatu islands. These values
227 are within the range of the data, even if the data tend to be slightly higher (up to 0.3 mg Chl.m⁻³ near the coasts). The spa-
228 tial structure is well represented, with maxima simulated around the islands. In the subtropical gyres, the simulation predicts
229 chlorophyll concentrations of 0.05 mg Chl.m⁻³ which are higher than in the observations (< 0.025 mg Chl.m⁻³). In contrast
230 in TRI_imp (Fig. 3c), chlorophyll values in the South West Pacific and in the North hemisphere are too low in comparison with
231 the ocean colour data (Fig. 3a).

232 Part of the surface chlorophyll in Figure 3b is associated with *Trichodesmium*. Figure 3d shows the annual mean spatial distri-
233 bution of surface *Trichodesmium* chlorophyll in the TRI simulation. This distribution displays two zonal tongues in the tropics,
234 one in each hemisphere. Maximum values are located in the South West Pacific (around Vanuatu archipelago, New Caledonia,
235 Fiji, and Papua New Guinea(PNG)) and around Hawaii, where they reach 0.06 mg Chl.m⁻³. In the South Pacific, high chloro-
236 phyll biomass extends eastward until 130°W. Further east, concentrations drop to below 0.02 mg Chl.m⁻³. It is important to
237 note that, in the observations, *Trichodesmium* have never been observed eastward of 170°W. This bias in the model could be
238 explained by the overestimated iron concentrations in the South Pacific Gyre (SPG). In the Northern Hemisphere, between
239 the coasts of Philippines (120°E) and Hawaii (140°W), *Trichodesmium* chlorophyll concentrations are greater than 0.03 mg
240 Chl.m⁻³. In the North East Pacific, *Trichodesmium* chlorophyll is lower, yet significant (<0.03 mg Chl.m⁻³). Otherwise the
241 equatorial Pacific and South East Pacific oceans are overall poor in *Trichodesmium*.

242 In Figure 4, the dinitrogen fixation rates predicted by the model in TRI are compared to the observations from the MAREDAT
243 expanded database. Evaluation of the model behavior remains quite challenging because of the scarcity of the observations.
244 Some large areas are not properly sampled such as the north west tropical Pacific and the eastern Pacific. In addition, some
245 areas are sampled only in the surface layer (0-30m), while others have been sampled deeper. This non-homogeneous sam-
246 pling may alter the distribution of the N₂ fixation rates and undermine the comparison with model outputs. To overcome this
247 sampling bias we compared the observations with N₂ fixation rates simulated integrated over two different layers (0-30m and
248 0-150m). Despite their scarcity, some regional patterns emerge from the observations. Maximum fixation rates (600 to 1600

249 $\mu\text{mol N.m}^{-2}.\text{d}^{-1}$; Fig. 4a) are observed around the south west Pacific islands, in the Solomon Sea, around the Melanesian
250 archipelagos and around Hawaii, four well known « hotspots » of N_2 fixation (Berthelot et al., 2015b, 2017; Bonnet et al.,
251 2009, 2017; Böttjer et al., 2017). The modeled regional patterns of strong fixation are coherent with the observations (Fig.
252 4b), showing values in the same range. In the south Pacific, the TRI simulation is able to reproduce the strong east-west in-
253 creasing gradient of N_2 fixation (Shiozaki et al., 2014; Bonnet et al., This issue; Fig 4c,d). In the equatorial Central Pacific,
254 modeled values of mean fixation are negligible ($< 0.5 \mu\text{mol N.m}^{-2}.\text{d}^{-1}$) in contrast to the observations which suggest low but
255 non-negligible fixation rates (between 1 to 2 $\mu\text{mol N.m}^{-2}.\text{d}^{-1}$) (Bonnet et al., 2009; Halm et al., 2012). On the whole mod-
256 eled domain and for both integration layers, dinitrogen fixation rates are overestimated by 70% in TRI compared to the data.
257 Some recent studies have shown that the 15N_2 -tracer addition method (Montoya et al., 2004) used in most studies reported
258 in the MAREDAT database may underestimate N_2 fixation rates due to an incomplete equilibration of the 15N_2 tracer in the
259 incubation bottles. Thus, this overestimation may be an artifact arising from methodological issues (Großkopf et al., 2012;
260 Mohr et al., 2010). However, some other studies performed in the South Pacific (Bonnet et al., 2016b; Shiozaki et al., 2015)
261 compared the two methods, and did not find any significant differences.

262 3.2 *Trichodesmium* Primary Production

263 We evaluated the direct relative contribution of *Trichodesmium* to PP (Fig. 5). The spatial distribution of this contribution
264 is very similar to the spatial distribution of *Trichodesmium* chlorophyll, with 2 distinct tongues located on each side of the
265 Equator in the tropical domain. In the Northern hemisphere, the tongue extends from the coast of Philippines (120°E) to
266 Hawaii (140°W) longitudinally and between 10°N and 25°N latitudinally. The maximum contribution (35%) is reached near
267 Hawaii while in the rest of the tongue, values are close to 20%. In the Southern Hemisphere, the region of elevated contribution
268 extends from PNG (140°E) to about the center of the South Pacific subtropical gyre at 130°W, and between 5°S and 25°S
269 latitudinally. Maximum values are predicted in the vicinity of Vanuatu and Fiji Islands, where they can reach 35%. Part of
270 this elevated contribution is explained by the very low PP rates simulated in this region for both nanophytoplankton and
271 diatoms (less than $0.03 \text{ mol C.m}^{-3}.\text{yr}^{-1}$). Furthermore, the island effect seems to represent an important factor for explaining
272 the spatial distribution of *Trichodesmium* growth rates. Indeed, maximum *Trichodesmium* chlorophyll concentrations and the
273 largest contribution of *Trichodesmium* to PP are achieved near the islands. Finally, in LNLC regions (red boxes; fig. 1c,d), we
274 assess that *Trichodesmium* contribute to 15% of total PP, which is in accordance with biogeochemical studies performed in
275 these areas (Bonnet et al., 2015; Berthelot et al., 2017; Caffin et al., This issue)

276 3.3 Seasonal variability of *Trichodesmium* biomass

277 *Trichodesmium* biomass (Fig. 6) and simulated dinitrogen fixation rates (Fig. 7) display a seasonal variability that is driven
278 by the seasonal variability of the environmental conditions (light, temperature, currents, nutrients). The regional maxima of
279 *Trichodesmium* biomass (exceeding 3 mmol C.m^{-2} ; integrated over the top 100m of the ocean) are found in both hemispheres
280 during the summer season (Fig. 6a,b) even if locally, maxima can be attained during other periods of the year than summer. In
281 the south Pacific, the area of elevated *Trichodesmium* biomass moves by 3° southward from austral winter to austral summer.

282 Along Australia and in the Coral Sea, *Trichodesmium* biomass exhibits a large seasonal variability with a very low winter
283 biomass that contrasts with elevated values in summer. A similar important variability, which is shifted by six months, is
284 simulated in the Northern hemisphere in the Micronesia region and in the Philippine Sea.

285 Unfortunately, due to the scarcity of N₂ fixation data, this seasonal cycle cannot be properly assessed at the scale of the tropical
286 Pacific Ocean. This is only feasible at the time series station ALOHA located in the North Pacific gyre at 22°45', 158°W,
287 where seasonal data of dinitrogen fixation are available from 2005 to 2012 (Böttjer et al., 2017). They proved that vertically
288 integrated dinitrogen fixation rates are statistically significantly (one-way ANOVA, p<0.01) lower from November to March
289 (less than 200 μmol N.m⁻².d⁻¹) than from April to October (about 263 ± 147 μmol N.m⁻².d⁻¹) as highlighted in Figure
290 7a (blue dots). In the model (red dots; Fig. 7a), the maximum amplitude of the seasonal cycle appears to be underestimated
291 relative to the observations (i.e. respectively 170 μmol N.m⁻².d⁻¹ and 250 μmol N.m⁻².d⁻¹). Dinitrogen fixation peaks one
292 month earlier in the model than in the data (August for the model and September for the data). Indeed, the simulated dinitrogen
293 fixation rates are minimum between December and May (averaging 241 ± 27 μmol N.m⁻².d⁻¹) and maximum the rest of the
294 year (averaging 347 ± 52 μmol N.m⁻².d⁻¹). These values are comparable to the data even if they are slightly higher.

295 In order to assess the seasonal cycle of N₂ fixation rates in the south Pacific (red box Fig 1c; 160°E-230°E; 25°S-14°S), we have
296 extracted the available data for each month from our database (blue dots; Fig. 7b), and the corresponding model values in TRI
297 (red dots; Fig 7b). In July no observations are available and in January, April and August, only one data point is available for the
298 entire region. The predicted seasonal cycle is broadly consistent with the observations. Minimum dinitrogen fixation rates (239
299 ± 205 μmol N.m⁻².d⁻¹) occur during austral winter and autumn. Maximum rates are reached in February and March, where
300 they exceed 600 μmol N.m⁻².d⁻¹ in the observations. The increase in dinitrogen fixations rates occurs one month earlier than
301 in the observations, in December instead of January, and remains two to three fold higher from April to June. It is important
302 to note here that the sampling spatial and temporal distribution may distort the seasonal cycle. Using the model, it is possible
303 to evaluate how well the seasonal cycle is captured by the sampling (red dots compared to green dots; Figure 7b). The general
304 structure of the seasonal cycle remains relatively unaltered. However, the amplitude is significantly impacted since it reaches
305 1100 μmol N.m⁻².d⁻¹ if sampled at the observed stations whereas it is about twice as low at 600 μmol N.m⁻².d⁻¹ if all the
306 model data points are considered. We can conclude that the TRI simulation reproduces well the seasonal cycle of N₂ fixation
307 rates at the Pacific scale, even though more data are needed to improve the evaluation of the model skills.

308 To further investigate the mechanisms that drive the seasonal variability of *Trichodesmium* in the Pacific, we examined the
309 factors that control *Trichodesmium* abundance in the TRI simulation (not shown). This decomposition shows that the physical
310 terms (advection and mixing) are negligible compared to biological terms. In addition, the seasonal cycles of grazing and
311 mortality are in phase with the production terms but their sign is opposite. In conclusion, this analysis indicates that this
312 seasonal variability is mainly controlled by the levels of primary production, the others terms of tracer evolution dampen its
313 amplitude but do not change its shape. Hence we further examine the limitation terms of primary production (Fig. 8) in two
314 representative regions characterized by elevated levels of N₂ fixation rates (red boxes; Fig 1c). A detailed description of these
315 limitation terms is given in Appendix 1. A limitation term reaching 1 means that growth is not limited whereas a limitation
316 term equal to zero means that growth ceases.

317 *Trichodesmium* growth sustained by nitrate and ammonia is very small in LNLC regions due to their very low availability
318 and is therefore not considered further. Thus, our analysis is restricted to dinitrogen fixation. *Trichodesmium* growth can be
319 limited by iron and phosphate and is inhibited when reactive nitrogen (nitrate and ammonia) is available. In the WTSP, the
320 model suggests that iron is the sole nutrient that modulates *Trichodesmium* growth (red curve; Fig. 8a,b). The others limiting
321 factors of *Trichodesmium* growth are light (green curve; Fig 8a,b) and temperature (purple curve; Fig. 8a,b). The product of
322 these 3 limiting factors gives the limiting coefficient of dinitrogen fixation (brown curve; Fig 8a,b). The limiting factors vary
323 according to the season and the hemisphere. In the south (north) Pacific, temperature and light are less limiting during the
324 austral summer (winter) than during the austral winter (summer). The limiting factor associated to temperature varies from
325 0.8 to 1, and the light limiting factor varies from 0.15 to 0.3. Unlike light and temperature, iron is less (more) limiting in the
326 south (north) Pacific during winter (summer) than during the austral summer (winter) with values varying between 0.4 and 0.7.
327 Finally, *Trichodesmium* growth is more limited during the austral winter (summer) in the south (north) Pacific. The seasonal
328 variability is forced by light and temperature, and iron mitigates its amplitude. Indeed, nutrients and iron inputs brought to the
329 euphotic zone by the seasonally enhanced vertical mixing are counter-balanced by the related inputs (e.g temperature) of these
330 water masses.

331 **4 Discussion**

332 **4.1 Impact of iron from island sediments**

333 Monteiro et al. (2011) performed a sensitivity study and found that a fivefold increase in the solubility of aeolian iron improves
334 the biogeographical distribution of N_2 fixation in the southwest Pacific. In the meantime, a recent study has challenged this
335 view by showing no increase in N_2 fixation in response to increased dust deposition (Luo et al., 2014). In any cases, the
336 sedimentary and hydrothermal sources were not taken into account in those studies, although they are likely significant sources
337 (Bennett et al., 2008; Johnson et al., 1999; Moore et al., 2004; Tagliabue et al., 2010; Toner et al., 2009). In parallel, Dutkiewicz
338 et al. (2012) evaluated the sensitivity of the biogeographical distribution of N_2 fixation to the aeolian source of iron in a model
339 which takes into account the iron sediment supplies, and conclude for minor changes in the south west Pacific, while in the
340 north Pacific the change was larger. Indeed, there are many islands with a marked orography that could deliver significant
341 amounts of iron to the ocean (Radic et al., 2011) in the southwest Pacific.

342 To assess the impact of the sediment source of iron on the *Trichodesmium* production, we used the «TRI_NoFeSed» experiment
343 in which this specific source of iron has been turned off for the islands between 156°E and 120°W (Table 1). In this simulation,
344 iron and *Trichodesmium* chlorophyll decrease by 58% and 51% respectively (Fig. 9a,b), in the WTSP (red box Fig 1c). Figure
345 9c displays the iron distribution simulated in TRI_NoFeSed, and shows that the maximums around the islands disappear.
346 Furthermore, in the south Pacific, iron decreases due to the reduction of the zonal advection of iron downstream of the islands.
347 The iron flux from the sediments around the islands also affects the spatial structure of *Trichodesmium* chlorophyll (Fig.
348 9e,f), most noticeably in the south Pacific, with maxima shifted from the south Pacific islands region (e.g. Fiji, New Caledonia,
349 Vanuatu) in the TRI simulation to the coastal regions near Australia and Papua New Guinea in the TRI_NoFeSed simulation. In

350 the northern hemisphere, the effects of the sediment flux of iron are less important with a shift of the *Trichodesmium* chlorophyll
351 maxima towards the Philippine Sea and a localized effect near Hawaii. This sensitivity test demonstrates that *Trichodesmium*
352 are highly sensitive to the iron distribution in our model and hence that the spatial patterns of *Trichodesmium* chlorophyll in
353 the south west Pacific are tightly controlled by the release of iron from the coastal sediments of the Pacific islands.

354 4.2 *Trichodesmium* impacts on biogeochemistry

355 One of the questions we want to address is the quantification of the *Trichodesmium* impact on primary production (PP), at
356 the Pacific scale with a focus on the WTSP region. In the oligotrophic waters of the south pacific, dinitrogen fixation can
357 be an important source of bio-available nitrogen in the water column through *Trichodesmium* recycling which can feed other
358 phytoplankton. To evaluate that impact, we calculated the relative increase of PP between the TRI simulation and the N₂_Wo
359 simulation in which no N₂ fixation is considered (Fig 10a). As expected, the spatial structure of the primary production differ-
360 ences between both simulations matches the N₂ fixation spatial distribution in the TRI simulation (two tongues, one in each
361 hemisphere). In the north Pacific the maximum increase of the primary production due to the N₂ fixation is located around
362 Hawaii, where it exceeds 120%. In the remaining part of the northern hemisphere tongue, primary production increases by
363 50% to 100%. In the southern hemisphere, values are more homogeneous in the tongue (from 80 to 100%), even though there
364 is a local maximum around Fiji and Vanuatu (up to 120%). Out of these northern and southern tongues, the increase of PP is
365 less than 20%. In average on our domain, the increase of PP is 19% and in LNL regions, it reaches approximately 50%.

366 From total primary production only, it is not possible to disentangle the increase of primary production directly due to *Tri-*
367 *chodesmium* themselves and the indirect increase due to the impact of N₂ fixation on the other phytoplankton groups (nanophy-
368 toplankton and diatoms). Indeed, as mentioned in the method section, *Trichodesmium* also releases a fraction of the recently
369 fixed N₂ as bio-available nitrogen (in our model *Trichodesmium* releases ammonia and dissolved organic nitrogen, but only
370 ammonia is directly bio-available). Figure 10b displays the difference in PP due to diatoms and nanophytoplankton only. The
371 main large scale patterns constituted of the northern and southern tongues persist, but the intensity of the differences contrasts
372 with those found when considering total primary production (Fig. 10a). Indeed, the increase of total primary production (Fig
373 10a) in those two tongues is twice as high as when the direct effect of *Trichodesmium* is excluded. This analysis stresses the
374 importance of the bio-available nitrogen released by diazotrophs as we attribute about half of the total production increase to
375 this release. Indeed, recent isotopic studies tracing the passage of diazotroph-derived nitrogen into the planktonic food web
376 reveal that part of the recently fixed nitrogen is released to the dissolved pool and quickly taken up (24-48%) by surrounding
377 planktonic communities (Berthelot et al., 2016; Bonnet et al., 2016b, a).

378 With the simulation TRI_imp, we aim at comparing an implicit N₂ fixation formulation to the explicit formulation used in TRI.
379 Figure 10c displays the relative change of total PP between the TRI and the TRI_imp simulations (see Table 2). The implicit
380 formulation displays a similar spatial distribution to that of the explicit distribution but it is predicting a lower total primary
381 production, especially in the the southern Pacific where explicit formulation leads to an increase of about 45% in total PP
382 compared to the one related to the implicit formulation. On average across our domain, total primary production is about 9%
383 higher when nitrogen fixation is explicitly modeled relative to an implicit formulation.

384 This difference becomes even weaker (2%) if only primary production by nanophytoplankton and diatoms is considered, with
385 noticeable differences restricted to the areas of maximum N_2 fixation in the southern hemisphere (around the islands). PP
386 sustained by the release of bio-available nitrogen is thus similar in the TRI and TRI_imp simulations, but an explicit represen-
387 tation of N_2 fixation allows a better description of N_2 fixation patterns. Indeed, the areas of intense N_2 fixation rates cannot be
388 properly simulated in the vicinity of the islands, especially in the southern hemisphere, by the tested implicit parameterization.
389 We also assessed the carbon export (under the euphotic layer, $\text{mmol C}\cdot\text{s}^{-2}\cdot\text{d}^{-1}$; Supp. Figure 1) and the N_2 fixation rate (inte-
390 grated over top to 150m; Supp. Figure 2: panel a in $\mu\text{mol N}\cdot\text{m}^{-2}\cdot\text{d}^{-1}$ and panel b in percentage) difference between TRI and
391 TRI_imp simulations. We observe a carbon export greater in TRI simulation, the average across the Pacific of this difference is
392 $0.1 \text{ mmol C}\cdot\text{m}^{-2}\cdot\text{d}^{-1}$ or 4 %, and in LNLC regions the increase varies between 6 and 10 %. The N_2 fixation rates are greater
393 in TRI simulation except in the warm pool, in the equatorial upwelling, and in Peru upwelling.

394 4.3 Limitations of the present study

395 In this study, we simulate N_2 fixation through the explicit representation of only one type of diazotrophs, the *Trichodesmium*
396 sp. This choice has been motivated by evidences that it represents one of the main nitrogen fixers in the western tropical Pacific
397 (Bonnet et al., 2015a; Dupouy et al., 2011; Shiozaki et al., 2014) and by the relatively good knowledge (compared to other
398 dinitrogen fixers) we have about its physiology (Ramamurthy and Krishnamurthy, 1967; Ohki et al., 1992; Mulholland and
399 Capone, 2000; Mulholland et al., 2001; Küpper et al., 2008; Rubin et al., 2011; Bergman et al., 2013). However, our model
400 remains simple and some of the mechanisms that drive the behavior of *Trichodesmium* have not been implemented in our model.
401 As an example, the ability of *Trichodesmium* to group in colonies and to vertically migrate (Kromkamp and Walsby, 1992;
402 Villareal and Carpenter, 2003; Bergman et al., 2013) is well documented. The reason of these mechanisms remains unclear,
403 but several hypotheses have been put forward such as avoiding nitrogenase exposition to di-oxygen (Carpenter, 1972; Gallon,
404 1992; Paerl et al., 1989), or maximizing light (on the surface) and nutrients (at depth) acquisition (Letelier and Karl, 1998;
405 Villareal and Carpenter, 1990; White et al., 2006), or even increasing the efficiency of the uptake of atmospheric iron (Rubin
406 et al., 2011). Our model does not represent those processes, nor does it model the resulting vertical migration of *Trichodesmium*.
407 Moreover, the release of fixed dinitrogen as reactive nitrogen bioavailable to other phytoplanktonic organisms has been set to
408 a constant value of 5%. This percentage is known to be highly variable and therefore this value is in the lowest range of the
409 observations. An increase in this value would increase the PP due to nanophytoplankton and diatoms in the TRI simulation, and
410 thus decrease the relative contribution of *Trichodesmium* to total PP, which would be closer to the last observations (Berthelot
411 et al., 2017; Bonnet et al., 2017).

412 Some studies, mostly based on extrapolated in-situ data, aimed at assessing the potential of N_2 fixation at global or regional
413 scale (Codispoti et al., 2001; Deutsch et al., 2001; Galloway et al., 2004). In the western south tropical Pacific, Bonnet et al
414 (2017) have estimated total N_2 fixation at 15 to 19 $\text{Tg N}\cdot\text{yr}^{-1}$. For the same region, N_2 fixation is predicted to amount to 7
415 $\text{Tg N}\cdot\text{yr}^{-1}$ in the TRI simulation. As already mentioned, this rather low predicted estimates might be explained by the sole
416 representation of *Trichodesmium* as nitrogen fixing organisms, which dominate in the western tropical south Pacific (Dupouy et
417 al., 2011, Stenegren et al., This issue). It has to be noted that other diazotroph groups such UCYN-B and DDAs are abundant in

418 the WTSP, representing 10-20% of the overall diazotroph community (Stenegren et al., This issue). Moreover, the contribution
419 of heterotrophic diazotrophic organism is poorly studied and may account for a significant fraction of N_2 fixation (Moisander
420 et al., 2017). Our model estimation has also been computed from monthly averages and is thus not taking into account the
421 high-frequency variability that may explain at least some of the very high rates of N_2 fixation found in the study by Bonnet et
422 al. (2017). Our assessment based on a model could thus be seen as a lower limit for N_2 fixation in the western tropical Pacific.
423 Moreover, our model shows also a good qualitative agreement with the studies based on observations that focus on the impact
424 of N_2 fixation in tropical oligotrophic waters (Raimbault and Garcia, 2008; Shiozaki et al., 2013). Indeed, in agreement with
425 those studies, our reference simulation predicts that diazotrophs support a significant part of total PP (15%) in LNLC regions.

426 **5 Conclusion**

427 This study describes the spatial and temporal distribution of *Trichodesmium* at the scale of the tropical Pacific ocean, and
428 investigates the impact of a major diazotroph species (e.g *Trichodesmium* sp.) on the biogeochemistry of this region. Toward
429 this end, we performed a first 20-year simulation with the coupled 3D dynamical biogeochemical model ROMS-PISCES in
430 which we embedded an explicit representation of N_2 fixation based on *Trichodesmium* physiology. This simulation was shown
431 to be able to reproduce the main physical (SST) and biogeochemical (nutrients) conditions of the tropical Pacific ocean. This
432 includes the spatial distribution of surface chlorophyll and N_2 fixation.

433 The validation of this simulation allows us to confidently assess the *Trichodesmium* distribution. The model predicts that areas
434 favorable to *Trichodesmium* growth extend from 150°E to 120°W in the south Pacific, and from 120°E to 140°W in the north
435 Pacific, with local optimal conditions around the islands (i.e., Hawaii, Fiji, Samoa, New Caledonia, Vanuatu). This broadly cor-
436 responds to the LNLC regions where *Trichodesmium* are predicted to be responsible for 15% of total primary production. The
437 seasonal variability of the *Trichodesmium* habitat is dominantly controlled by SST and light, while iron availability modulates
438 the amplitude of the seasonal cycle.

439 In our study we also assess the role played by iron released from the island sediments, and show that this iron source partly
440 controls the spatial structure and the abundance of *Trichodesmium* in the western tropical south Pacific. However, this region is
441 in the center of the south Pacific convergence zone which is the largest convective area of the Southern Hemisphere, with rain-
442 fall exceeding 6 mm.day^{-1} , hence it would be interesting to assess the impact of river iron supply on the diazotrophs activity.
443 In addition, the Vanuatu archipelago and Tonga are located on the ring fire, hence hydrothermal sources could have a strong
444 impact on N_2 fixation. These two iron sources are not yet implemented in our configuration but may improve simulations of N_2
445 fixation in the south western tropical Pacific region. Finally, our explicit simulation of N_2 fixation has proven to be higher by
446 25% (while still in the lower end of estimations from observations) than the more commonly used implicit parameterization.

447 **6 Appendix**

448 *Trichodesmium* preferentially fixes N₂ at temperature between 20-34°C (Breitbarth et al., 2007). The temperature effect on the
449 growth rate is modeled using a 4th order polynomial function (Ye et al., 2012):

$$450 L_T^{Tri} = \frac{2,32.10^{-5} \times T^4 - 2,52.10^{-3} \times T^3 + 9,75.10^{-2} \times T^2 - 1,58 \times T + 9,12}{0,25} \quad (3)$$

451 where 0.25d⁻¹ is the maximum observed growth rate (Breitbarth et al., 2007). Hence, at 17°C the growth rate is zero and
452 maximum growth rate is reached at 27°C. The *Trichodesmium* light limitation is similar to nanophytoplankton (Aumont et al.
453 (2015)).

454 From equation 2, we distinguish 2 cases for the growth rate due to N₂ fixation.

455 If phosphorus is limiting the equation 2 becomes :

$$456 \mu_{FixN_2} = \mu_{max}^{Tri} \cdot L_I^{Tri} \cdot L_P^{Tri} - (\mu_{NO_3}^{Tri} + \mu_{NH_4}^{Tri}) \text{ with,} \quad (4a)$$

$$457 L_P^{Tri} = \min \left(1, \max \left(0, \frac{(\theta^P - \theta_{min}^P) \times \theta_{max}^P}{(\theta_{max}^P - \theta_{min}^P) \times \theta^P} \right) \right) \quad (4b)$$

458

459 if iron is limiting :

$$460 \mu_{FixN_2} = \mu_{max}^{Tri} \cdot L_I^{Tri} \cdot L_{Fe}^{Tri} - (\mu_{NO_3}^{Tri} + \mu_{NH_4}^{Tri}) \text{ with,} \quad (5a)$$

$$461 L_{Fe}^{Tri} = \min \left(1, \max \left(0, \frac{(\theta^{Fe} - \theta_1^{Fe}) \times \theta_{opt}^{Fe}}{(\theta_{opt}^{Fe} - \theta_0^{Fe}) \times \theta^{Fe}} \right) \right) \quad (5b)$$

462

463 In equation 5b, θ_1^{Fe} and θ_0^{Fe} are computed as follows :

$$464 \theta_1^{Fe} = \theta_0^{Fe} + \alpha \cdot \mu_{FixN_2} \quad (6a)$$

$$465 \theta_0^{Fe} = \theta_{min}^{Fe} + m \quad (6b)$$

$$466 \alpha = \frac{1}{\beta} \quad (6c)$$

467 $\theta^{Nutrients}$ represents the nutrient quota for Fe and phosphorus (i.e, the ratio between iron and carbon concentrations in *Tri-*
468 *chodesmium*, for instance). θ_{min}^P , and θ_{opt}^{Fe} are constants, whereas $\theta^{Nutrients}$ varies with time. The minimum between L_{Fe}^{Tri}
469 and L_P^{Tri} defines the limiting nutrient. L_I^{Tri} is the limiting function by temperature and light. m is the difference between the
470 maintenance iron (i.e, the intracellular Fe:C present in the cell at zero growth rate) for a diazotrophic growth and a growth on
471 ammonium (Kustka et al., 2003). β is the marginal use efficiency and equals the moles of additional carbon fixed per additional
472 mole of intracellular iron per day (Raven, 1988; Sunda and Huntsman, 1997). The demands for iron in phytoplankton are for
473 photosynthesis, respiration and nitrate/nitrite reduction. Following Flynn et al. (1997), we assume that the rate of synthesis by
474 the cell of new components requiring iron is given by the difference between the iron quota and the sum of the iron required

475 by these three sources of demand, which we defined as the actual minimum iron quota:

$$476 \theta_{min}^{Fe} = \frac{0,0016}{55,85} \theta_{Tri}^{Chl} + \frac{1,21 \cdot 10^{-5} \times 14}{55,85 \times 7,625} L_N^{Tri} \times 1,5 + \frac{1,15 \cdot 10^{-4} \times 14}{55,85 \times 7,625} L_{NO_3}^{Tri} \quad (7)$$

477 In this equation, the first right term corresponds to photosynthesis, the second term corresponds to respiration and the third
478 term estimates nitrate and nitrite reduction. The parameters used in this equation are directly taken from Flynn and Hipkin
479 (1999).

480 *Acknowledgements.* We thank the ship captains, the scientists as well as funding agencies of all the projects (OUTPACE, BIOSOPE, MOOR-
481 SPICE, DIAPALIS, NECTALIS, PANDORA, Mirai) that allowed data collection without which we could not validate our model. The authors
482 thank Institute of Research for Development for supporting all authors. Cyril Dutheil is funded by European project INTEGRÉ.

483 References

- 484 Arrigo, K. R.: Marine microorganisms and global nutrient cycles, *Nature*, 437, 349–355, <https://doi.org/10.1038/nature04159>, <http://www.nature.com/articles/nature04159>, 2005.
- 485
- 486 Assmann, K. M., Bentsen, M., Segschneider, J., and Heinze, C.: An isopycnic ocean carbon cycle model, *Geoscientific Model Development*
- 487 *Discussions*, 2, 1023–1079, <https://doi.org/10.5194/gmdd-2-1023-2009>, <http://www.geosci-model-dev-discuss.net/2/1023/2009/>, 2009.
- 488 Aumont, O. and Bopp, L.: Globalizing results from ocean in situ iron fertilization studies: GLOBALIZING IRON FERTILIZATION, *Global*
- 489 *Biogeochemical Cycles*, 20, n/a–n/a, <https://doi.org/10.1029/2005GB002591>, <http://doi.wiley.com/10.1029/2005GB002591>, 2006.
- 490 Aumont, O., Ethé, C., Tagliabue, A., Bopp, L., and Gehlen, M.: PISCES-v2: an ocean biogeochemical model for carbon and ecosys-
- 491 *tem studies*, *Geoscientific Model Development Discussions*, 8, 1375–1509, <https://doi.org/10.5194/gmdd-8-1375-2015>, <http://www.geosci-model-dev-discuss.net/8/1375/2015/>, 2015.
- 492
- 493 Bennett, S. A., Achterberg, E. P., Connelly, D. P., Statham, P. J., Fones, G. R., and German, C. R.: The distribution
- 494 and stabilisation of dissolved Fe in deep-sea hydrothermal plumes, *Earth and Planetary Science Letters*, 270, 157–167,
- 495 <https://doi.org/10.1016/j.epsl.2008.01.048>, <http://linkinghub.elsevier.com/retrieve/pii/S0012821X08001003>, 2008.
- 496 Bergman, B., Sandh, G., Lin, S., Larsson, J., and Carpenter, E. J.: *Trichodesmium* – a widespread marine cyanobacterium with un-
- 497 *usual nitrogen fixation properties*, *FEMS Microbiology Reviews*, 37, 286–302, <https://doi.org/10.1111/j.1574-6976.2012.00352.x>, <https://academic.oup.com/femsre/article-lookup/doi/10.1111/j.1574-6976.2012.00352.x>, 2013.
- 498
- 499 Berman-Frank, I.: Segregation of Nitrogen Fixation and Oxygenic Photosynthesis in the Marine Cyanobacterium *Trichodesmium*, *Science*,
- 500 294, 1534–1537, <https://doi.org/10.1126/science.1064082>, <http://www.sciencemag.org/cgi/doi/10.1126/science.1064082>, 2001.
- 501 Berthelot, H., Bonnet, S., Camps, M., Grosso, O., and Moutin, T.: Assessment of the dinitrogen released as ammonium and dissolved
- 502 *organic nitrogen by unicellular and filamentous marine diazotrophic cyanobacteria grown in culture*, *Frontiers in Marine Science*, 2,
- 503 <https://doi.org/10.3389/fmars.2015.00080>, <http://journal.frontiersin.org/Article/10.3389/fmars.2015.00080/abstract>, 2015a.
- 504 Berthelot, H., Moutin, T., L’Helguen, S., Leblanc, K., Hélias, S., Grosso, O., Leblond, N., Charrière, B., and Bonnet, S.: Dinitrogen fixation
- 505 and dissolved organic nitrogen fueled primary production and particulate export during the VAHINE mesocosm experiment (New Cale-
- 506 *donia lagoon)*, *Biogeosciences*, 12, 4099–4112, <https://doi.org/10.5194/bg-12-4099-2015>, <http://www.biogeosciences.net/12/4099/2015/>,
- 507 2015b.
- 508 Berthelot, H., Bonnet, S., Grosso, O., Cornet, V., and Barani, A.: Transfer of diazotroph-derived nitrogen towards non-diazotrophic planktonic
- 509 *communities: a comparative study between *Trichodesmium erythraeum*, *Crocospaera watsonii* and *Cyanothece* sp.*, *Biogeosciences*, 13,
- 510 4005–4021, <https://doi.org/10.5194/bg-13-4005-2016>, <http://www.biogeosciences.net/13/4005/2016/>, 2016.
- 511 Berthelot, H., Benavides, M., Moisander, P. H., Grosso, O., and Bonnet, S.: High-nitrogen fixation rates in the particulate and dissolved
- 512 *pools in the Western Tropical Pacific (Solomon and Bismarck Seas): N₂ Fixation in the Western Pacific*, *Geophysical Research Letters*,
- 513 44, 8414–8423, <https://doi.org/10.1002/2017GL073856>, <http://doi.wiley.com/10.1002/2017GL073856>, 2017.
- 514 Bissett, W., Walsh, J., Dieterle, D., and Carder, K.: Carbon cycling in the upper waters of the Sargasso Sea: I. Numerical simulation of differ-
- 515 *ential carbon and nitrogen fluxes*, *Deep Sea Research Part I: Oceanographic Research Papers*, 46, 205–269, [https://doi.org/10.1016/S0967-](https://doi.org/10.1016/S0967-0637(98)00062-4)
- 516 [0637\(98\)00062-4](http://linkinghub.elsevier.com/retrieve/pii/S0967063798000624), <http://linkinghub.elsevier.com/retrieve/pii/S0967063798000624>, 1999.
- 517 Bombar, D., Paerl, R. W., and Riemann, L.: Marine Non-Cyanobacterial Diazotrophs: Moving beyond Molecular Detection, *Trends in*
- 518 *Microbiology*, 24, 916–927, <https://doi.org/10.1016/j.tim.2016.07.002>, <http://linkinghub.elsevier.com/retrieve/pii/S0966842X16300889>,
- 519 2016.

520 Bonnet, S., Biegala, I. C., Dutrieux, P., Slemons, L. O., and Capone, D. G.: Nitrogen fixation in the western equatorial Pacific: Rates,
521 diazotrophic cyanobacterial size class distribution, and biogeochemical significance: N₂ fixation in the equatorial Pacific, *Global Biogeo-*
522 *chemical Cycles*, 23, n/a–n/a, <https://doi.org/10.1029/2008GB003439>, <http://doi.wiley.com/10.1029/2008GB003439>, 2009.

523 Bonnet, S., Rodier, M., Turk-Kubo, K. A., Germineaud, C., Menkes, C., Ganachaud, A., Cravatte, S., Raimbault, P., Campbell, E., Quéroué,
524 F., Sarthou, G., Desnues, A., Maes, C., and Eldin, G.: Contrasted geographical distribution of N₂ fixation rates and *nif* H phylotypes
525 in the Coral and Solomon Seas (southwestern Pacific) during austral winter conditions: N₂ fixation and diversity in the Pacific, *Global*
526 *Biogeochemical Cycles*, 29, 1874–1892, <https://doi.org/10.1002/2015GB005117>, <http://doi.wiley.com/10.1002/2015GB005117>, 2015.

527 Bonnet, S., Berthelot, H., Turk-Kubo, K., Cornet-Barthaux, V., Fawcett, S., Berman-Frank, I., Barani, A., Grégori, G., Dekaezemacker, J., Be-
528 navides, M., and Capone, D. G.: Diazotroph derived nitrogen supports diatom growth in the South West Pacific: A quantitative study using
529 nanoSIMS: Transfer of diazotrophic N into plankton, *Limnology and Oceanography*, 61, 1549–1562, <https://doi.org/10.1002/lno.10300>,
530 <http://doi.wiley.com/10.1002/lno.10300>, 2016a.

531 Bonnet, S., Berthelot, H., Turk-Kubo, K., Fawcett, S., Rahav, E., & Helguen, S., and Berman-Frank, I.: Dynamics of N₂ fixation and fate
532 of diazotroph-derived nitrogen in a low-nutrient, low-chlorophyll ecosystem: results from the VAHINE mesocosm experiment (New Cale-
533 donia), *Biogeosciences*, 13, 2653–2673, <https://doi.org/10.5194/bg-13-2653-2016>, <http://www.biogeosciences.net/13/2653/2016/>, 2016b.

534 Bonnet, S., Caffin, M., Berthelot, H., and Moutin, T.: Hot spot of N₂ fixation in the western tropical South Pacific pleads for a spatial
535 decoupling between N₂ fixation and denitrification, *Proceedings of the National Academy of Sciences*, 114, E2800–E2801, 2017.

536 Breitbarth, E., Oschlies, A., and Laroche, J.: Physiological constraints on the global distribution of *Trichodesmium*? effect of temperature
537 on diazotrophy, *Biogeosciences*, 4, 53–61, <https://hal.archives-ouvertes.fr/hal-00297595>, 2007.

538 Breitbarth, E., Wohlers, J., Kläs, J., LaRoche, J., and Peeken, I.: Nitrogen fixation and growth rates of *Trichodesmium* IMS-101 as a func-
539 tion of light intensity, *Marine Ecology Progress Series*, 359, 25–36, <https://doi.org/10.3354/meps07241>, [http://www.int-res.com/abstracts/](http://www.int-res.com/abstracts/meps/v359/p25-36/)
540 [meps/v359/p25-36/](http://www.int-res.com/abstracts/meps/v359/p25-36/), 2008.

541 Böttjer, D., Dore, J. E., Karl, D. M., Letelier, R. M., Mahaffey, C., Wilson, S. T., Zehr, J., and Church, M. J.: Temporal variability of nitrogen
542 fixation and particulate nitrogen export at Station ALOHA: Temporal variability of nitrogen fixation and particulate nitrogen, *Limnology*
543 *and Oceanography*, 62, 200–216, <https://doi.org/10.1002/lno.10386>, <http://doi.wiley.com/10.1002/lno.10386>, 2017.

544 Capone, D. G.: *Trichodesmium*, a Globally Significant Marine Cyanobacterium, *Science*, 276, 1221–1229,
545 <https://doi.org/10.1126/science.276.5316.1221>, <http://www.sciencemag.org/cgi/doi/10.1126/science.276.5316.1221>, 1997.

546 Carpenter, E. J.: Nitrogen Fixation by a Blue-Green Epiphyte on Pelagic Sargassum, *Science*, 178, 1207–1209,
547 <https://doi.org/10.1126/science.178.4066.1207>, <http://www.sciencemag.org/cgi/doi/10.1126/science.178.4066.1207>, 1972.

548 Church, M. J., Jenkins, B. D., Karl, D. M., and Zehr, J. P.: Vertical distributions of nitrogen-fixing phylotypes at Stn ALOHA in the olig-
549 otrophic North Pacific Ocean, *Aquatic Microbial Ecology*, 38, 3–14, 2005.

550 Codispoti, L. A., Brandes, J. A., Christensen, J. P., Devol, A. H., Naqvi, S. A., Paerl, H. W., and Yoshinari, T.: The
551 oceanic fixed nitrogen and nitrous oxide budgets: Moving targets as we enter the anthropocene?, *Scientia Marina*, 65, 85–105,
552 <https://doi.org/10.3989/scimar.2001.65s285>, <http://scientiamarina.revistas.csic.es/index.php/scientiamarina/article/view/684/700>, 2001.

553 Couvelard, X., Marchesiello, P., Gourdeau, L., and Lefèvre, J.: Barotropic Zonal Jets Induced by Islands in the Southwest Pacific,
554 *Journal of Physical Oceanography*, 38, 2185–2204, <https://doi.org/10.1175/2008JPO3903.1>, [http://journals.ametsoc.org/doi/abs/10.1175/](http://journals.ametsoc.org/doi/abs/10.1175/2008JPO3903.1)
555 [2008JPO3903.1](http://journals.ametsoc.org/doi/abs/10.1175/2008JPO3903.1), 2008.

556 Cravatte, S., Madec, G., Izumo, T., Menkes, C., and Bozec, A.: Progress in the 3-D circulation of the eastern equatorial Pacific in a cli-
557 mate ocean model, *Ocean Modelling*, 17, 28–48, <https://doi.org/10.1016/j.ocemod.2006.11.003>, [http://linkinghub.elsevier.com/retrieve/](http://linkinghub.elsevier.com/retrieve/pii/S1463500306001119)
558 [pii/S1463500306001119](http://linkinghub.elsevier.com/retrieve/pii/S1463500306001119), 2007.

559 Da Silva, A. M., Young, C., and Levitus, S.: Algorithms and Procedures, in: *Atlas of Surface Marine Data*, vol. 1, p. 83, noaa atlas nesdis
560 edn., 1994.

561 Daines, S. J., Clark, J. R., and Lenton, T. M.: Multiple environmental controls on phytoplankton growth strategies determine adaptive
562 responses of the N : P ratio, *Ecology Letters*, 17, 414–425, <https://doi.org/10.1111/ele.12239>, <http://doi.wiley.com/10.1111/ele.12239>,
563 2014.

564 Delmont, T. O., Quince, C., Shaiber, A., Esen, O. C., Lee, S. T. M., Lucker, S., and Eren, A. M.: Nitrogen-Fixing Populations Of Plancto-
565 mycetes And Proteobacteria Are Abundant In The Surface Ocean, pp. –, <https://doi.org/10.1101/129791>, <http://biorxiv.org/lookup/doi/10.1101/129791>, 2017.

567 Deutsch, C., Gruber, N., Key, R. M., Sarmiento, J. L., and Ganachaud, A.: Denitrification and N₂ fixation in the Pacific Ocean, *Global*
568 *Biogeochemical Cycles*, 15, 483–506, <https://doi.org/10.1029/2000GB001291>, <http://doi.wiley.com/10.1029/2000GB001291>, 2001.

569 Deutsch, C., Sarmiento, J. L., Sigman, D. M., Gruber, N., and Dunne, J. P.: Spatial coupling of nitrogen inputs and losses in the ocean,
570 *Nature*, 445, 163–167, <https://doi.org/10.1038/nature05392>, <http://www.nature.com/doi/10.1038/nature05392>, 2007a.

571 Deutsch, C., Sarmiento, J. L., Sigman, D. M., Gruber, N., and Dunne, J. P.: Spatial coupling of nitrogen inputs and losses in the ocean,
572 *Nature*, 445, 163–167, <https://doi.org/10.1038/nature05392>, <http://www.nature.com/articles/nature05392>, 2007b.

573 Dunne, J. P., JOHN, J. G., SHEVLIAKOVA, E., STOUFFER, R. J., KRASTING, J. P., MALYSHEV, S. L., MILLY, P. C. D., SENTMAN,
574 L. T., ADCROFT, A. J., COOKE, W., DUNNE, K. A., GRIFFIES, S. M., HALLBERG, R. W., HARRISON, M. J., LEVY, H., WITTEN-
575 BERG, A. T., PHILLIPS, P. J., and ZADEH, N.: GFDL’s ESM2 Global Coupled Climate–Carbon Earth System Models. Part II: Carbon
576 System Formulation and Baseline Simulation Characteristics, *Journal of Climate*, 26, 21, 2013.

577 Dupouy, C., Neveux, J., Subramaniam, A., Mulholland, M. R., Montoya, J. P., Campbell, L., Carpenter, E. J., and Capone, D. G.: Satel-
578 lite captures trichodesmium blooms in the southwestern tropical Pacific, *Eos, Transactions American Geophysical Union*, 81, 13,
579 <https://doi.org/10.1029/00EO00008>, <http://doi.wiley.com/10.1029/00EO00008>, 2000.

580 Dupouy, C., Benielli-Gary, D., Neveux, J., Dandonneau, Y., and Westberry, T. K.: An algorithm for detecting Trichodesmium surface blooms
581 in the South Western Tropical Pacific, *Biogeosciences*, 8, 3631–3647, <https://hal-sde.archives-ouvertes.fr/hal-00875926/>, 2011.

582 Dutkiewicz, S., Ward, B. A., Monteiro, F., and Follows, M. J.: Interconnection of nitrogen fixers and iron in the Pacific Ocean: Theory and nu-
583 merical simulations: marine nitrogen fixers and iron, *Global Biogeochemical Cycles*, 26, n/a–n/a, <https://doi.org/10.1029/2011GB004039>,
584 <http://doi.wiley.com/10.1029/2011GB004039>, 2012.

585 Falcón, L. I., Pluvinage, S., and Carpenter, E. J.: Growth kinetics of marine unicellular N-fixing cyanobacterial isolates in continuous culture
586 in relation to phosphorus and temperature, *Marine Ecology Progress Series*, 285, 3–9, 2005.

587 Fennel, K., Spitz, Y. H., Letelier, R. M., Abbott, M. R., and Karl, D. M.: A deterministic model for N₂ fixation at stn. ALOHA in the
588 subtropical North Pacific Ocean, *Deep Sea Research Part II: Topical Studies in Oceanography*, 49, 149–174, 2001.

589 Flynn, K. J., Fasham, M. J., and Hipkin, C. R.: Modelling the interactions between ammonium and nitrate uptake in marine phytoplankton,
590 *Philosophical Transactions of the Royal Society of London B: Biological Sciences*, 352, 1625–1645, [http://rstb.royalsocietypublishing.](http://rstb.royalsocietypublishing.org/content/352/1361/1625.short)
591 [org/content/352/1361/1625.short](http://rstb.royalsocietypublishing.org/content/352/1361/1625.short), 1997.

592 Gallon, J. R.: Reconciling the incompatible: N₂ fixation And O₂, *New Phytologist*, 122, 571–609, [https://doi.org/10.1111/j.1469-](https://doi.org/10.1111/j.1469-8137.1992.tb00087.x)
593 [8137.1992.tb00087.x](http://doi.wiley.com/10.1111/j.1469-8137.1992.tb00087.x), <http://doi.wiley.com/10.1111/j.1469-8137.1992.tb00087.x>, 1992.

594 Galloway, J. N., Dentener, F. J., Capone, D. G., Boyer, E. W., Howarth, R. W., Seitzinger, S. P., Asner, G. P., Cleveland, C. C., Green, P. A.,
595 Holland, E. A., Karl, D. M., Michaels, A. F., Porter, J. H., Townsend, A. R., and Vörösmarty, C. J.: Nitrogen Cycles: Past, Present, and Fu-
596 ture, *Biogeochemistry*, 70, 153–226, <https://doi.org/10.1007/s10533-004-0370-0>, <http://link.springer.com/10.1007/s10533-004-0370-0>,
597 2004.

598 Garcia, N., Raimbault, P., and Sandroni, V.: Seasonal nitrogen fixation and primary production in the Southwest Pacific:
599 nanoplankton diazotrophy and transfer of nitrogen to picoplankton organisms, *Marine Ecology Progress Series*, 343, 25–33,
600 <https://doi.org/10.3354/meps06882>, <http://www.int-res.com/abstracts/meps/v343/p25-33/>, 2007.

601 Goebel, N. L., Edwards, C. A., Carter, B. J., Achilles, K. M., and Zehr, J. P.: Growth and carbon content of three different-sized dia-
602 zotrophic cyanobacteria observed in the subtropical north pacific, *Journal of Phycology*, 44, 1212–1220, <https://doi.org/10.1111/j.1529->
603 [8817.2008.00581.x](http://doi.wiley.com/10.1111/j.1529-8817.2008.00581.x), <http://doi.wiley.com/10.1111/j.1529-8817.2008.00581.x>, 2008.

604 Großkopf, T., Mohr, W., Baustian, T., Schunck, H., Gill, D., Kuypers, M. M. M., Lavik, G., Schmitz, R. A., Wallace, D. W. R., and LaRoche,
605 J.: Doubling of marine dinitrogen-fixation rates based on direct measurements, *Nature*, 488, 361–364, <https://doi.org/10.1038/nature11338>,
606 <http://www.nature.com/doi/10.1038/nature11338>, 2012.

607 Gruber, N.: Oceanography: A bigger nitrogen fix, *Nature*, 436, 786–787, 2005.

608 Gruber, N.: The Marine Nitrogen Cycle: Overview and challenges, in: *Nitrogen in the Marine Environment*, pp. 1–50, Elsevier,
609 <https://doi.org/10.1016/B978-0-12-372522-6.00001-3>, <http://linkinghub.elsevier.com/retrieve/pii/B9780123725226000013>, 2008.

610 Halm, H., Lam, P., Ferdelman, T. G., Lavik, G., Dittmar, T., LaRoche, J., D’Hondt, S., and Kuypers, M. M.: Heterotrophic organisms
611 dominate nitrogen fixation in the South Pacific Gyre, *The ISME Journal*, 6, 1238–1249, <https://doi.org/10.1038/ismej.2011.182>, <http://www.nature.com/doi/10.1038/ismej.2011.182>, 2012.

612

613 Hawser, S. P., O’neil, J. M., Roman, M. R., and Codd, G. A.: Toxicity of blooms of the cyanobacterium *Trichodesmium* to zooplankton,
614 *Journal of Applied Phycology*, 4, 79–86, 1992.

615 Hood, R. R., Bates, N. R., Capone, D. G., and Olson, D. B.: Modeling the effect of nitrogen fixation on carbon and nitrogen fluxes at
616 BATS, Deep Sea Research Part II: Topical Studies in Oceanography, 48, 1609–1648, [https://doi.org/10.1016/S0967-0645\(00\)00160-0](https://doi.org/10.1016/S0967-0645(00)00160-0),
617 <http://linkinghub.elsevier.com/retrieve/pii/S0967064500001600>, 2001.

618 Johnson, K. S., Chavez, F. P., and Friederich, G. E.: Continental-shelf sediment as a primary source of iron for coastal phytoplankton, *Nature*,
619 398, 697–700, <https://doi.org/10.1038/19511>, <http://www.nature.com/articles/19511>, 1999.

620 Jullien, S., Menkes, C. E., Marchesiello, P., Jourdain, N. C., Lengaigne, M., Koch-Larrouy, A., Lefèvre, J., Vincent, E. M., and Faure,
621 V.: Impact of Tropical Cyclones on the Heat Budget of the South Pacific Ocean, *Journal of Physical Oceanography*, 42, 1882–1906,
622 <https://doi.org/10.1175/JPO-D-11-0133.1>, <http://journals.ametsoc.org/doi/abs/10.1175/JPO-D-11-0133.1>, 2012.

623 Jullien, S., Marchesiello, P., Menkes, C. E., Lefèvre, J., Jourdain, N. C., Samson, G., and Lengaigne, M.: Ocean feedback to tropical cyclones:
624 climatology and processes, *Climate Dynamics*, 43, 2831–2854, <https://doi.org/10.1007/s00382-014-2096-6>, [http://link.springer.com/10.](http://link.springer.com/10.1007/s00382-014-2096-6)
625 [1007/s00382-014-2096-6](http://link.springer.com/10.1007/s00382-014-2096-6), 2014.

626 Karl, D., Letelier, R., Tupas, L., Dore, J., Christian, J., and Hebel, D.: The role of nitrogen fixation in biogeochemical cycling in the subtropical
627 North Pacific Ocean, *Nature*, 388, 533–538, 1997.

628 Keith Moore, J., Doney, S. C., Lindsay, K., Mahowald, N., and Michaels, A. F.: Nitrogen fixation amplifies the ocean biogeochemi-
629 cal response to decadal timescale variations in mineral dust deposition, *Tellus B: Chemical and Physical Meteorology*, 58, 560–572,
630 <https://doi.org/10.1111/j.1600-0889.2006.00209.x>, <https://www.tandfonline.com/doi/full/10.1111/j.1600-0889.2006.00209.x>, 2006.

631 Kessler, W. S. and Gourdeau, L.: The Annual Cycle of Circulation of the Southwest Subtropical Pacific, Analyzed in an Ocean GCM*, Journal
632 of Physical Oceanography, 37, 1610–1627, <https://doi.org/10.1175/JPO3046.1>, <http://journals.ametsoc.org/doi/abs/10.1175/JPO3046.1>,
633 2007.

634 Klausmeier, C. A., Litchman, E., Daufresne, T., and Levin, S. A.: Optimal nitrogen-to-phosphorus stoichiometry of phytoplankton, Nature,
635 429, 171–174, <https://doi.org/10.1038/nature02454>, <http://www.nature.com/doi/finder/10.1038/nature02454>, 2004.

636 Krishnamurthy, A., Moore, J. K., Mahowald, N., Luo, C., Doney, S. C., Lindsay, K., and Zender, C. S.: Impacts of increasing anthropogenic
637 soluble iron and nitrogen deposition on ocean biogeochemistry: atmospheric Fe and N and ocean biogeochemistry, Global Biogeochemical
638 Cycles, 23, n/a–n/a, <https://doi.org/10.1029/2008GB003440>, <http://doi.wiley.com/10.1029/2008GB003440>, 2009.

639 Kromkamp, J. and Walsby, A. E.: Buoyancy Regulation and Vertical Migration of Trichodesmium: a Computer-Model Prediction, in: Marine
640 Pelagic Cyanobacteria: Trichodesmium and other Diazotrophs, edited by Carpenter, E. J., Capone, D. G., and Rueter, J. G., pp. 239–248,
641 Springer Netherlands, Dordrecht, https://doi.org/10.1007/978-94-015-7977-3_15, http://link.springer.com/10.1007/978-94-015-7977-3_15,
642 1992.

643 Kustka, A. B., Sanudo-Wilhelmy, S. A., Carpenter, E. J., Capone, D., Burns, J., and Sunda, W. G.: Iron requirements for dinitrogen-and
644 ammonium-supported growth in cultures of Trichodesmium (IMS 101): Comparison with nitrogen fixation rates and iron: carbon ratios of
645 field populations, Limnology and Oceanography, 48, 1869–1884, http://www-ccd.usc.edu/assets/sites/125/docs/Kustka_et_al_2003_LO.pdf, 2003.

647 Kwiatkowski, L., Aumont, O., Bopp, L., and Ciais, P.: The Impact of Variable Phytoplankton Stoichiometry on Projections of
648 Primary Production, Food Quality, and Carbon Uptake in the Global Ocean, Global Biogeochemical Cycles, 32, 516–528,
649 <https://doi.org/10.1002/2017GB005799>, <http://doi.wiley.com/10.1002/2017GB005799>, 2018.

650 Küpper, H., etlk, I., Seibert, S., Pril, O., etlikova, E., Strittmatter, M., Levitan, O., Lohscheider, J., Adamska, I., and Berman-Frank, I.: Iron
651 limitation in the marine cyanobacterium *Trichodesmium* reveals new insights into regulation of photosynthesis and nitrogen fixation, New
652 Phytologist, 179, 784–798, <https://doi.org/10.1111/j.1469-8137.2008.02497.x>, <http://doi.wiley.com/10.1111/j.1469-8137.2008.02497.x>,
653 2008.

654 Large, W. G., McWilliams, J. C., and Doney, S. C.: Oceanic vertical mixing: A review and a model with a nonlocal boundary layer parame-
655 terization, Reviews of Geophysics, 32, 363, <https://doi.org/10.1029/94RG01872>, <http://doi.wiley.com/10.1029/94RG01872>, 1994.

656 LaRoche, J. and Breitbarth, E.: Importance of the diazotrophs as a source of new nitrogen in the ocean, Journal of Sea Research, 53, 67–91,
657 <https://doi.org/10.1016/j.seares.2004.05.005>, <http://linkinghub.elsevier.com/retrieve/pii/S1385110104000930>, 2005.

658 Letelier, R. and Karl, D.: Trichodesmium spp. physiology and nutrient fluxes in the North Pacific subtropical gyre, Aquatic Microbial
659 Ecology, 15, 265–276, <https://doi.org/10.3354/ame015265>, <http://www.int-res.com/abstracts/ame/v15/n3/p265-276/>, 1998.

660 Luo, Y.-W., Doney, S. C., Anderson, L. A., Benavides, M., Berman-Frank, I., Bode, A., Bonnet, S., Boström, K. H., Böttjer, D., Capone,
661 D. G., Carpenter, E. J., Chen, Y. L., Church, M. J., Dore, J. E., Falcón, L. I., Fernández, A., Foster, R. A., Furuya, K., Gómez, F.,
662 Gundersen, K., Hynes, A. M., Karl, D. M., Kitajima, S., Langlois, R. J., LaRoche, J., Letelier, R. M., Marañón, E., McGillicuddy, D. J.,
663 Moisander, P. H., Moore, C. M., Mouriño-Carballido, B., Mulholland, M. R., Needoba, J. A., Orcutt, K. M., Poulton, A. J., Rahav, E.,
664 Raimbault, P., Rees, A. P., Riemann, L., Shiozaki, T., Subramaniam, A., Tyrrell, T., Turk-Kubo, K. A., Varela, M., Villareal, T. A., Webb,
665 E. A., White, A. E., Wu, J., and Zehr, J. P.: Database of diazotrophs in global ocean: abundance, biomass and nitrogen fixation rates, Earth
666 System Science Data, 4, 47–73, <https://doi.org/10.5194/essd-4-47-2012>, <http://www.earth-syst-sci-data.net/4/47/2012/>, 2012.

667 Luo, Y.-W., Lima, I. D., Karl, D. M., Deutsch, C. A., and Doney, S. C.: Data-based assessment of environmental controls on global marine
668 nitrogen fixation, *Biogeosciences*, 11, 691–708, <https://doi.org/10.5194/bg-11-691-2014>, <http://www.biogeosciences.net/11/691/2014/>,
669 2014.

670 Maier-Reimer, E., Kriest, I., Segschneider, J., and Wetzol, P.: The Hamburg Ocean Carbon Cycle Model HAMOCC5 -Technical Description
671 Release 1.1-, Reports on earth system science, 14, http://eprints.uni-kiel.de/14321/1/erdsystem_14.pdf, 2005.

672 Marchesiello, P., McWilliams, J. C., and Shchepetkin, A.: Open boundary conditions for long-term integration of regional
673 oceanic models, *Ocean Modelling*, 3, 1–20, [https://doi.org/10.1016/S1463-5003\(00\)00013-5](https://doi.org/10.1016/S1463-5003(00)00013-5), [http://linkinghub.elsevier.com/retrieve/pii/](http://linkinghub.elsevier.com/retrieve/pii/S1463500300000135)
674 [S1463500300000135](http://linkinghub.elsevier.com/retrieve/pii/S1463500300000135), 2001.

675 Marchesiello, P., Lefèvre, J., Vega, A., Couvelard, X., and Menkes, C.: Coastal upwelling, circulation and heat balance around New Cale-
676 donia's barrier reef, *Marine Pollution Bulletin*, 61, 432–448, <https://doi.org/10.1016/j.marpolbul.2010.06.043>, <http://linkinghub.elsevier.com/retrieve/pii/S0025326X10002869>, 2010.

677

678 Meunier, C. L., Malzahn, A. M., and Boersma, M.: A New Approach to Homeostatic Regulation: Towards a Unified View of Physiological
679 and Ecological Concepts, *PLoS ONE*, 9, e107737, <https://doi.org/10.1371/journal.pone.0107737>, [http://dx.plos.org/10.1371/journal.pone.](http://dx.plos.org/10.1371/journal.pone.0107737)
680 [0107737](http://dx.plos.org/10.1371/journal.pone.0107737), 2014.

681 Mills, M. M., Ridame, C., Davey, M., La Roche, J., and Geider, R. J.: Iron and phosphorus co-limit nitrogen fixation in the eastern tropical
682 North Atlantic, *Nature*, 429, 292–294, 2004.

683 Mohr, W., Großkopf, T., Wallace, D. W. R., and LaRoche, J.: Methodological Underestimation of Oceanic Nitrogen Fixation Rates, *PLoS*
684 *ONE*, 5, e12583, <https://doi.org/10.1371/journal.pone.0012583>, <http://dx.plos.org/10.1371/journal.pone.0012583>, 2010.

685 Moisaner, P. H., Beinart, R. A., Voss, M., and Zehr, J. P.: Diversity and abundance of diazotrophic microorganisms in the South China Sea
686 during intermonsoon, *The ISME journal*, 2, 954–967, 2008.

687 Moisaner, P. H., Beinart, R. A., Hewson, I., White, A. E., Johnson, K. S., Carlson, C. A., Montoya, J. P., and Zehr, J. P.: Unicellular
688 cyanobacterial distributions broaden the oceanic N₂ fixation domain, *Science*, 327, 1512–1514, [http://science.sciencemag.org/content/](http://science.sciencemag.org/content/327/5972/1512.short)
689 [327/5972/1512.short](http://science.sciencemag.org/content/327/5972/1512.short), 2010.

690 Moisaner, P. H., Benavides, M., Bonnet, S., Berman-Frank, I., White, A. E., and Riemann, L.: Chasing after Non-cyanobacterial Ni-
691 trogen Fixation in Marine Pelagic Environments, *Frontiers in Microbiology*, 8, <https://doi.org/10.3389/fmicb.2017.01736>, [http://journal.](http://journal.frontiersin.org/article/10.3389/fmicb.2017.01736/full)
692 [frontiersin.org/article/10.3389/fmicb.2017.01736/full](http://journal.frontiersin.org/article/10.3389/fmicb.2017.01736/full), 2017.

693 Monteiro, F. M., Dutkiewicz, S., and Follows, M. J.: Biogeographical controls on the marine nitrogen fixers: controls on marine nitrogen fix-
694 ers, *Global Biogeochemical Cycles*, 25, n/a–n/a, <https://doi.org/10.1029/2010GB003902>, <http://doi.wiley.com/10.1029/2010GB003902>,
695 2011.

696 Montoya, J. P., Holl, C. M., Zehr, J. P., Hansen, A., Villareal, T. A., and Capone, D. G.: High rates of N₂ fixation by unicellular diazotrophs in
697 the oligotrophic Pacific Ocean, *Nature*, 430, 1027–1032, <https://doi.org/10.1038/nature02824>, [http://www.nature.com/doifinder/10.1038/](http://www.nature.com/doifinder/10.1038/nature02824)
698 [nature02824](http://www.nature.com/doifinder/10.1038/nature02824), 2004.

699 Moore, C. M., Mills, M. M., Arrigo, K. R., Berman-Frank, I., Bopp, L., Boyd, P. W., Galbraith, E. D., Geider, R. J., Guieu, C., Jaccard, S. L.,
700 Jickells, T. D., La Roche, J., Lenton, T. M., Mahowald, N. M., Marañón, E., Marinov, I., Moore, J. K., Nakatsuka, T., Oschlies, A., Saito,
701 M. A., Thingstad, T. F., Tsuda, A., and Ulloa, O.: Processes and patterns of oceanic nutrient limitation, *Nature Geoscience*, 6, 701–710,
702 <https://doi.org/10.1038/ngeo1765>, <http://www.nature.com/doifinder/10.1038/ngeo1765>, 2013.

703 Moore, J. K., Doney, S. C., Kleypas, J. A., Glover, D. M., and Fung, I. Y.: An intermediate complexity marine ecosystem model for the
704 global domain, *Deep Sea Research Part II: Topical Studies in Oceanography*, 49, 403–462, 2001.

705 Moore, J. K., Doney, S. C., and Lindsay, K.: Upper ocean ecosystem dynamics and iron cycling in a global three-dimensional model: global
706 ecosystem-biogeochemical model, *Global Biogeochemical Cycles*, 18, n/a–n/a, <https://doi.org/10.1029/2004GB002220>, <http://doi.wiley.com/10.1029/2004GB002220>, 2004.

708 Moutin, T., Van Den Broeck, N., Beker, B., Dupouy, C., Rimmelin, P., and Le Bouteiller, A.: Phosphate availability controls *Trichodesmium*
709 spp. biomass in the SW Pacific Ocean, *Marine Ecology Progress Series*, 297, 15–21, [https://www.researchgate.net/profile/Cecile_](https://www.researchgate.net/profile/Cecile_Dupouy/publication/250218377_Phosphate_availability_controls_Trichodesmium_spp_biomass_in_the_SW_Pacific_Ocean/links/55d366bd08ae0b8f3ef92ce2.pdf)
710 [Dupouy/publication/250218377_Phosphate_availability_controls_Trichodesmium_spp_biomass_in_the_SW_Pacific_Ocean/links/](https://www.researchgate.net/profile/Cecile_Dupouy/publication/250218377_Phosphate_availability_controls_Trichodesmium_spp_biomass_in_the_SW_Pacific_Ocean/links/55d366bd08ae0b8f3ef92ce2.pdf)
711 [55d366bd08ae0b8f3ef92ce2.pdf](https://www.researchgate.net/profile/Cecile_Dupouy/publication/250218377_Phosphate_availability_controls_Trichodesmium_spp_biomass_in_the_SW_Pacific_Ocean/links/55d366bd08ae0b8f3ef92ce2.pdf), 2005.

712 Moutin, T., Karl, D. M., Duhamel, S., Rimmelin, P., Raimbault, P., Van Mooy, B. A. S., and Claustre, H.: Phosphate availabil-
713 ity and the ultimate control of new nitrogen input by nitrogen fixation in the tropical Pacific Ocean, *Biogeosciences*, 5, 95–109,
714 <https://doi.org/10.5194/bg-5-95-2008>, <http://www.biogeosciences.net/5/95/2008/>, 2008.

715 Mulholland, M. R. and Capone, D. G.: The nitrogen physiology of the marine N₂-fixing cyanobacteria *Trichodesmium* spp., *Trends in Plant*
716 *Science*, 5, 148–153, [https://doi.org/10.1016/S1360-1385\(00\)01576-4](https://doi.org/10.1016/S1360-1385(00)01576-4), <http://linkinghub.elsevier.com/retrieve/pii/S1360138500015764>,
717 2000.

718 Mulholland, M. R. and Capone, D. G.: Stoichiometry of nitrogen and carbon utilization in cultured populations of *Trichodesmium* IMS101:
719 Implications for growth, *Limnology and Oceanography*, 46, 436–443, 2001.

720 Neveux, J., Tenírio, M. M. B., Dupouy, C., and Villareal, T. A.: Spectral diversity of phycoerythrins and diazotroph abundance in tropical
721 waters, *Limnology and Oceanography*, 51, 1689–1698, <https://doi.org/10.4319/lo.2006.51.4.1689>, [http://doi.wiley.com/10.4319/lo.2006.](http://doi.wiley.com/10.4319/lo.2006.51.4.1689)
722 [51.4.1689](http://doi.wiley.com/10.4319/lo.2006.51.4.1689), 2006.

723 Ohki, K., Zehr, J. P., and Fujita, Y.: Regulation of nitrogenase activity in relation to the light-dark regime in the filamentous non-heterocystous
724 cyanobacterium *Trichodesmium* sp. NIBB 1067, *Microbiology*, 138, 2679–2685, 1992.

725 O’Neil, J. and Romane, M.: Grazers and Associated Organisms of *Trichodesmium*, in *Marine Pelagic Cyanobacteria: Trichodesmium and*
726 *other Diazotrophs*, vol. 362, Springer Netherlands, Dordrecht, <http://public.ebib.com/choice/publicfullrecord.aspx?p=3568440>, oCLC:
727 958543480, 1992.

728 Paerl, H. W., Priscu, J. C., and Brawner, D. L.: Immunochemical localization of nitrogenase in marine *Trichodesmium* aggregates: Relation-
729 ship to N₂ fixation potential, *Applied and environmental microbiology*, 55, 2965–2975, 1989.

730 Pahlow, M. and Oschlies, A.: Chain model of phytoplankton P, N and light colimitation, *Marine Ecology Progress Series*, 376, 69–83,
731 <https://doi.org/10.3354/meps07748>, <http://www.int-res.com/abstracts/meps/v376/p69-83/>, 2009.

732 Penven, P., Debreu, L., Marchesiello, P., and McWilliams, J. C.: Evaluation and application of the ROMS 1-way embedding procedure to
733 the central california upwelling system, *Ocean Modelling*, 12, 157–187, <https://doi.org/10.1016/j.ocemod.2005.05.002>, [http://linkinghub.](http://linkinghub.elsevier.com/retrieve/pii/S1463500305000491)
734 [elsevier.com/retrieve/pii/S1463500305000491](http://linkinghub.elsevier.com/retrieve/pii/S1463500305000491), 2006.

735 Postgate, J. R.: Biology nitrogen fixation: fundamentals, *Philosophical Transactions of the Royal Society of London B: Biological Sciences*,
736 296, 375–385, 1982.

737 Radic, A., Lacan, F., and Murray, J. W.: Iron isotopes in the seawater of the equatorial Pacific Ocean: New constraints for the oceanic iron
738 cycle, *Earth and Planetary Science Letters*, 306, 1–10, <https://doi.org/10.1016/j.epsl.2011.03.015>, [http://linkinghub.elsevier.com/retrieve/](http://linkinghub.elsevier.com/retrieve/pii/S0012821X11001592)
739 [pii/S0012821X11001592](http://linkinghub.elsevier.com/retrieve/pii/S0012821X11001592), 2011.

740 Raimbault, P. and Garcia, N.: Evidence for efficient regenerated production and dinitrogen fixation in nitrogen-deficient waters of the
741 South Pacific Ocean: impact on new and export production estimates, *Biogeosciences*, 5, 323–338, [https://hal.archives-ouvertes.fr/](https://hal.archives-ouvertes.fr/hal-00327638/)
742 [hal-00327638/](https://hal.archives-ouvertes.fr/hal-00327638/), 2008.

743 Ramamurthy, V. D. and Krishnamurthy, S.: Effects of N: P ratios on the uptake of nitrate and phosphate by laboratory cultures of Tri-
744 chodesmium erythraeum (Ehr.), *Proceedings: Plant Sciences*, 65, 43–48, 1967.

745 Raven, J. A.: The iron and molybdenum use efficiencies of plant growth with different energy, carbon and nitrogen sources, *New Phytologist*,
746 109, 279–287, <https://doi.org/10.1111/j.1469-8137.1988.tb04196.x>, <http://doi.wiley.com/10.1111/j.1469-8137.1988.tb04196.x>, 1988.

747 Rubin, M., Berman-Frank, I., and Shaked, Y.: Dust- and mineral-iron utilization by the marine dinitrogen-fixer *Trichodesmium*, *Nature*
748 *Geoscience*, 4, 529–534, <https://doi.org/10.1038/ngeo1181>, <http://www.nature.com/doi/10.1038/ngeo1181>, 2011.

749 Rueter, J. G.: Iron stimulation of photosynthesis and nitrogen fixation in *Anabaena* 7120 and *Trichodesmium* (Cyanophyceae), *Journal of*
750 *Phycology*, 24, 249–254, <https://doi.org/10.1111/j.1529-8817.1988.tb04240.x>, <http://doi.wiley.com/10.1111/j.1529-8817.1988.tb04240.x>,
751 1988.

752 Shchepetkin, A. F. and McWilliams, J. C.: The regional oceanic modeling system (ROMS): a split-explicit, free-surface, topography-
753 following-coordinate oceanic model, *Ocean Modelling*, 9, 347–404, <https://doi.org/10.1016/j.ocemod.2004.08.002>, <http://linkinghub.elsevier.com/retrieve/pii/S1463500304000484>, 2005.

755 Shiozaki, T., Kodama, T., Kitajima, S., Sato, M., and Furuya, K.: Advective transport of diazotrophs and importance of their ni-
756 trogen fixation on new and primary production in the western Pacific warm pool, *Limnology and Oceanography*, 58, 49–60,
757 <https://doi.org/10.4319/lo.2013.58.1.0049>, <http://doi.wiley.com/10.4319/lo.2013.58.1.0049>, 2013.

758 Shiozaki, T., Kodama, T., and Furuya, K.: Large-scale impact of the island mass effect through nitrogen fixation in the western South Pacific
759 Ocean: island mass effect through N₂ fixation, *Geophysical Research Letters*, 41, 2907–2913, <https://doi.org/10.1002/2014GL059835>,
760 <http://doi.wiley.com/10.1002/2014GL059835>, 2014.

761 Staal, M., Filip, Meysman, and Lucas: Temperature excludes N₂-fixing heterocystous cyanobacteria in the tropical oceans, *Nature*, 425,
762 501–504, <https://doi.org/10.1038/nature02001>, <http://www.nature.com/articles/nature02001>, 2003.

763 Sterner, R. W. and Elser, J. J.: *Ecological Stoichiometry: The Biology of Elements from Molecules to the Biosphere*, [https://doi.org/10.1515/](https://doi.org/10.1515/9781400885695)
764 [9781400885695](https://doi.org/10.1515/9781400885695), oCLC: 979781039, 2002.

765 Sunda, W. G. and Huntsman, S. A.: Interrelated influence of iron, light and cell size on marine phytoplankton growth, *Nature*, 390, 389–392,
766 <https://doi.org/10.1038/37093>, <http://www.nature.com/articles/37093>, 1997.

767 Tagliabue, A., Bopp, L., and Aumont, O.: Ocean biogeochemistry exhibits contrasting responses to a large scale reduction in dust deposition,
768 *Biogeosciences*, 5, 11–24, 2008.

769 Tagliabue, A., Bopp, L., Dutay, J.-C., Bowie, A. R., Chever, F., Jean-Baptiste, P., Bucciarelli, E., Lannuzel, D., Remenyi, T., Sarthou, G.,
770 Aumont, O., Gehlen, M., and Jeandel, C.: Hydrothermal contribution to the oceanic dissolved iron inventory, *Nature Geoscience*, 3,
771 252–256, <https://doi.org/10.1038/ngeo818>, <http://www.nature.com/doi/10.1038/ngeo818>, 2010.

772 Tegen, I. and Fung, I.: Contribution to the atmospheric mineral aerosol load from land surface modification, *Journal of Geophysical Research*,
773 100, 18 707, <https://doi.org/10.1029/95JD02051>, <http://doi.wiley.com/10.1029/95JD02051>, 1995.

774 Toner, B. M., Fakra, S. C., Manganini, S. J., Santelli, C. M., Marcus, M. A., Moffett, J. W., Rouxel, O., German, C. R., and
775 Edwards, K. J.: Preservation of iron(II) by carbon-rich matrices in a hydrothermal plume, *Nature Geoscience*, 2, 197–201,
776 <https://doi.org/10.1038/ngeo433>, <http://www.nature.com/doi/10.1038/ngeo433>, 2009.

777 Turk-Kubo, K. A., Karamchandani, M., Capone, D. G., and Zehr, J. P.: The paradox of marine heterotrophic nitrogen fixation: abundances
778 of heterotrophic diazotrophs do not account for nitrogen fixation rates in the Eastern Tropical South Pacific: N₂-fixing potential of
779 heterotrophs in the ETSP, *Environmental Microbiology*, 16, 3095–3114, <https://doi.org/10.1111/1462-2920.12346>, [http://doi.wiley.com/](http://doi.wiley.com/10.1111/1462-2920.12346)
780 [10.1111/1462-2920.12346](http://doi.wiley.com/10.1111/1462-2920.12346), 2014.

781 Villareal, T. and Carpenter, E.: Buoyancy Regulation and the Potential for Vertical Migration in the Oceanic Cyanobacterium *Trichodesmium*,
782 *Microbial Ecology*, 45, 1–10, <https://doi.org/10.1007/s00248-002-1012-5>, <http://link.springer.com/10.1007/s00248-002-1012-5>, 2003.

783 Villareal, T. A. and Carpenter, E. J.: Diel buoyancy regulation in the marine diazotrophic cyanobacterium *Trichodesmium thiebautii*, *Lim-*
784 *nology and Oceanography*, 35, 1832–1837, <https://doi.org/10.4319/lo.1990.35.8.1832>, <http://doi.wiley.com/10.4319/lo.1990.35.8.1832>,
785 1990.

786 White, A., Spitz, Y., and Letelier, R.: Modeling carbohydrate ballasting by *Trichodesmium* spp., *Marine Ecology Progress Series*, 323, 35–45,
787 <https://doi.org/10.3354/meps323035>, <http://www.int-res.com/abstracts/meps/v323/p35-45/>, 2006.

788 Ye, Y., Völker, C., Bracher, A., Taylor, B., and Wolf-Gladrow, D. A.: Environmental controls on N₂ fixation by *Trichodesmium* in the
789 tropical eastern North Atlantic Ocean—A model-based study, *Deep Sea Research Part I: Oceanographic Research Papers*, 64, 104–117,
790 <https://doi.org/10.1016/j.dsr.2012.01.004>, <http://linkinghub.elsevier.com/retrieve/pii/S0967063712000167>, 2012.

791 Zahariev, K., Christian, J. R., and Denman, K. L.: Preindustrial, historical, and fertilization simulations using a global ocean car-
792 bon model with new parameterizations of iron limitation, calcification, and N₂ fixation, *Progress in Oceanography*, 77, 56–82,
793 <https://doi.org/10.1016/j.pocean.2008.01.007>, <http://linkinghub.elsevier.com/retrieve/pii/S0079661108000104>, 2008.

794 Zehr, J. P. and Bombar, D.: Marine Nitrogen Fixation: Organisms, Significance, Enigmas, and Future Directions, in: *Biological Nitrogen Fix-*
795 *ation*, edited by de Bruijn, F. J., pp. 855–872, John Wiley & Sons, Inc, Hoboken, NJ, USA, <https://doi.org/10.1002/9781119053095.ch84>,
796 <http://doi.wiley.com/10.1002/9781119053095.ch84>, 2015.

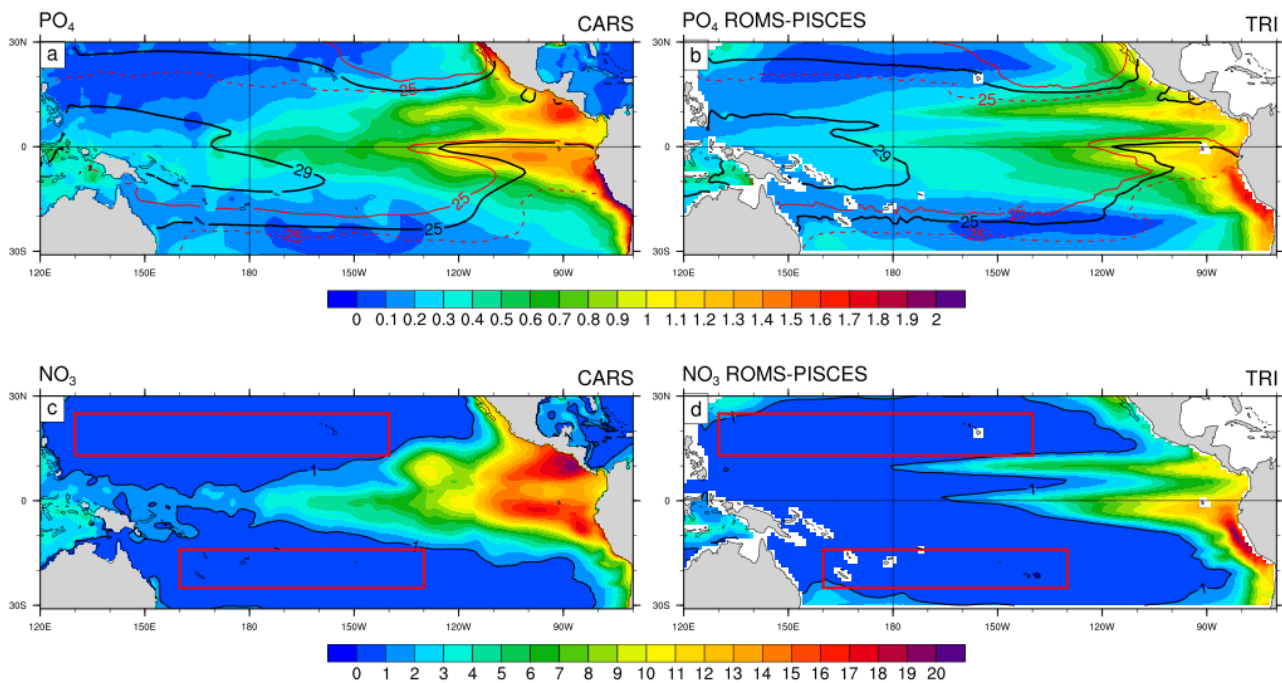


Figure 1. Annual mean concentrations in $\mu\text{mol.L}^{-1}$: a) PO_4 data from CARS b) PO_4 simulated by the ROMS-PISCES model c) NO_3 data from CARS d) NO_3 simulated by the ROMS-PISCES model. On panels (a) and (b), the black contours show the annual mean patterns of the temperature preferendum from observations (a) and the model (b). The red contours display the 25°C isolign in austral winter (plain) and in austral summer (dash). On panels (c) and (d) the red boxes represent the LNLC regions (defined as region where $[\text{NO}_3^-] < 1 \mu\text{mol.L}^{-1}$ and $[\text{Chl}] < 0.1 \text{ mg Chl.m}^{-3}$).

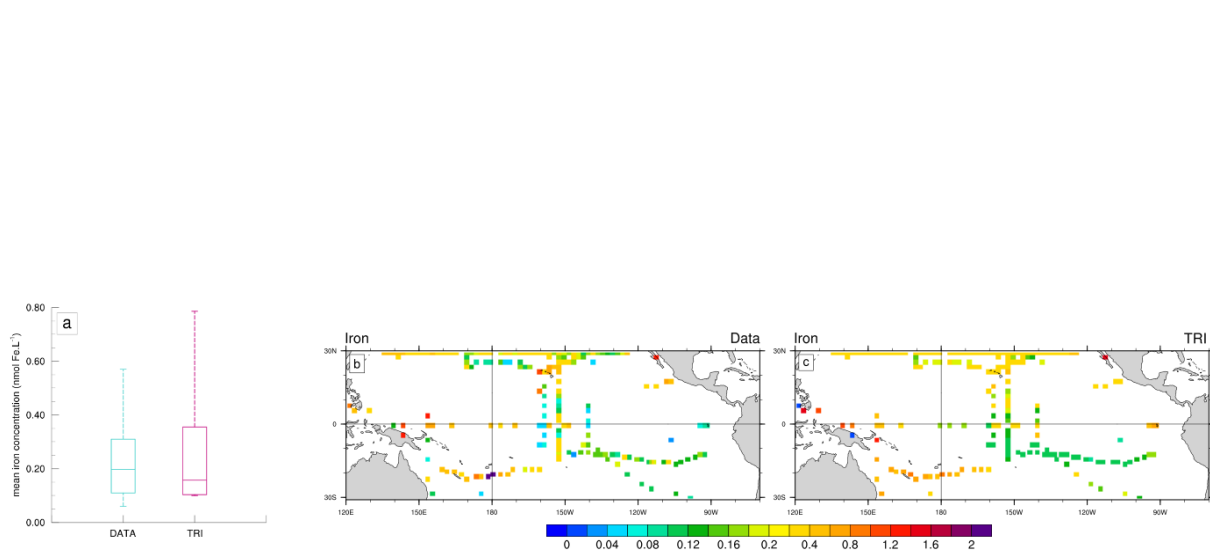


Figure 2. Left : Boxplots of the 0-150m averaged Iron (nmol Fe.L⁻¹) data (blue) and the equivalent for the model (red) colocalised with the observations in space and time. The coloured box represents the 25-75% quartile of the distribution, the whiskers the 10-90% percentile distribution. The line inside the coloured box is the median.

Right : Iron concentrations (nmol Fe.L⁻¹) as observed (b) and as simulated by the model (c). Iron concentrations have been averaged over the top 150m of the ocean. Model values have been sampled at the same location, the same month, and the same depth as the data.

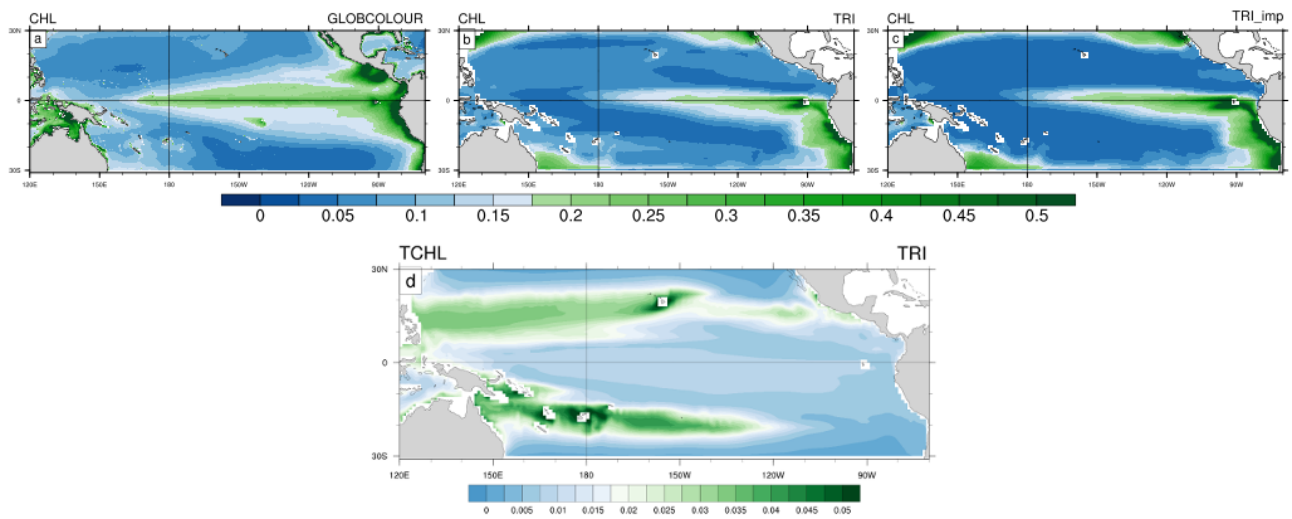


Figure 3. Top : Annual mean surface Chlorophyll concentrations (in mg Chl.m⁻³) from (a) GLOBCOLOUR data (b) TRI simulation and (c) TRI_imp simulation.

Bottom: panel (d) shows the the annual mean surface chlorophyll concentrations of *Trichodesmium* in the TRI simulation.

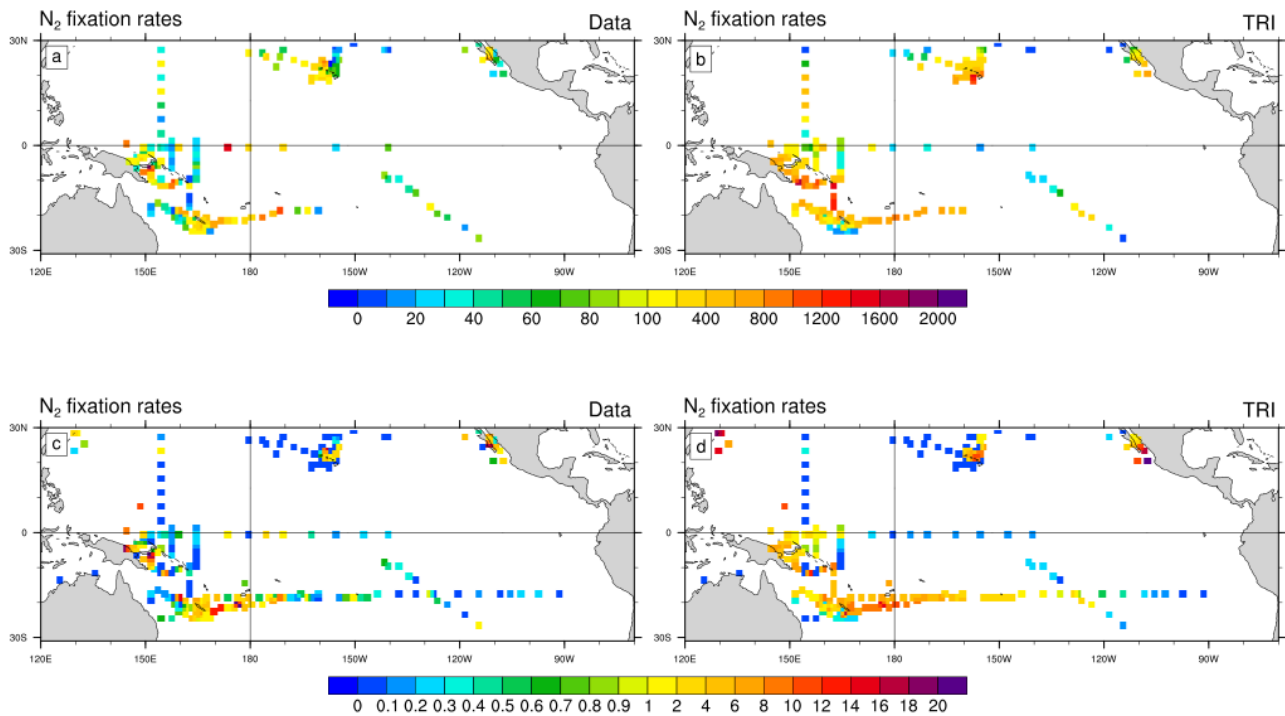


Figure 4. N_2 fixation rates ($\mu\text{mol N}\cdot\text{m}^{-2}\cdot\text{d}^{-1}$) as observed (left) and as simulated by TRI simulation (right). In the top panels, N_2 fixation rates have been integrated over the top 150m of the ocean. In the bottom panels, the vertical integration has been restricted to the top 30m of the ocean. Model values have been sampled at the same location, the same month (climatological month vs real month), and the same depth as the data.

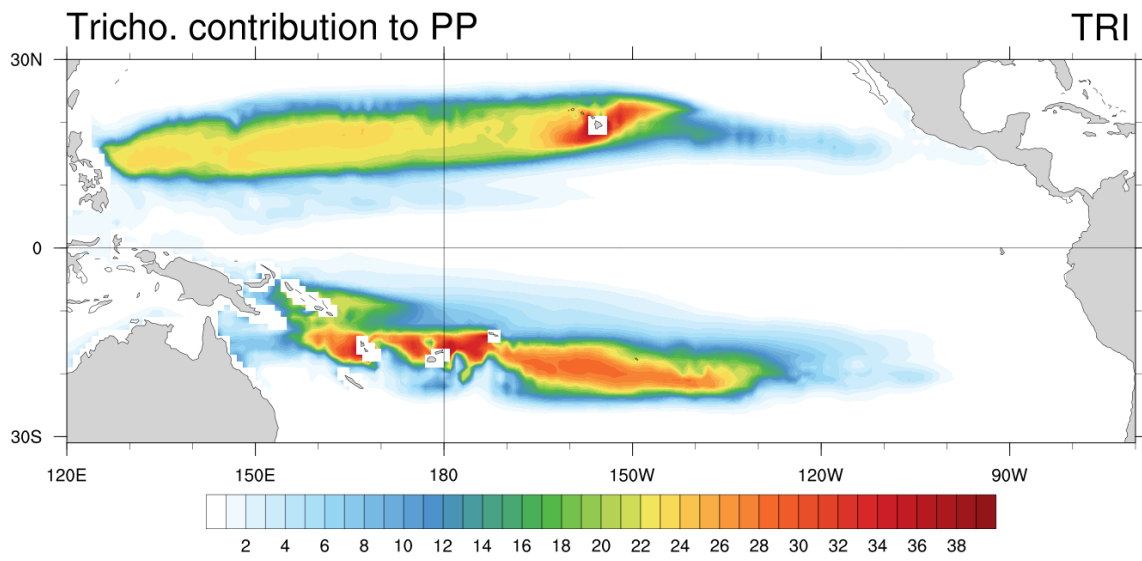


Figure 5. Relative contribution (in percentage) of *Trichodesmium* to total primary production.

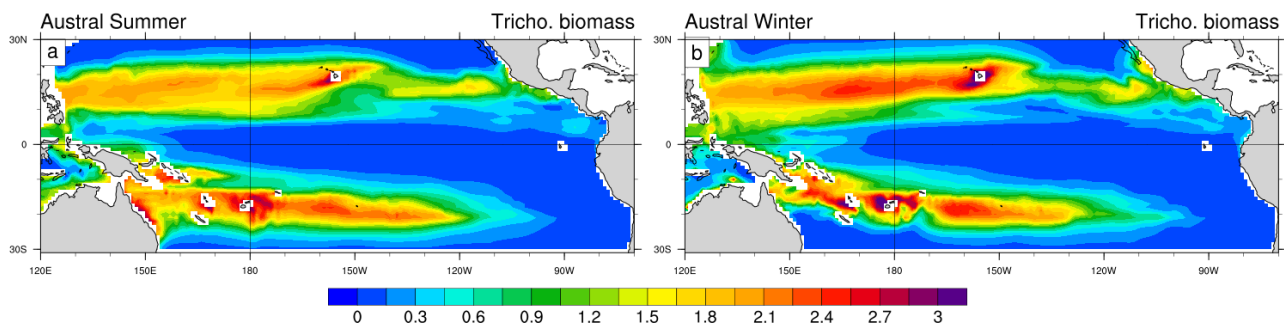


Figure 6. *Trichodesmium* biomass (mmol C.m^{-2}) in (a) austral summer and (b) austral winter, integrated over the top 100m of the ocean.

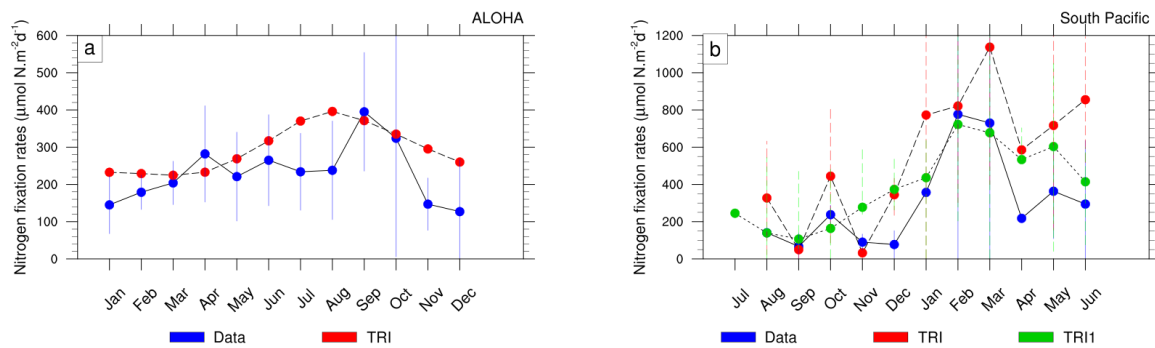


Figure 7. a) Depth-integrated (0 to 125m) rates of N_2 fixation ($\mu\text{mol N.m}^{-2}\text{.d}^{-1}$) at ALOHA for the data (blue) and TRI simulation (red). b) Depth-integrated (from 0 to 150m) rates of N_2 fixation ($\mu\text{mol N.m}^{-2}\text{.d}^{-1}$) in the south Pacific (red box, Fig. 1c) in the data (blue) and in the TRI simulation (red). The blue curve is the average of all the model points inside the south Pacific zone (red box, Fig. 1c), whereas the green curve corresponds to the average of the model points where data are available.

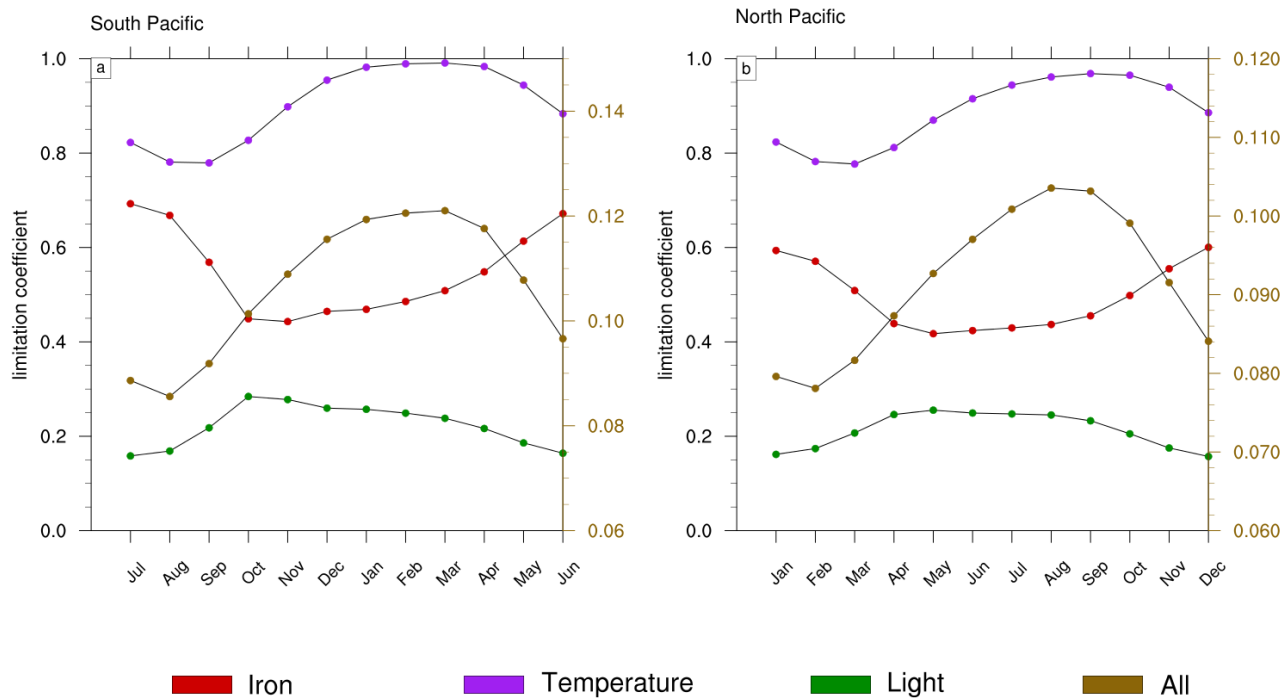


Figure 8. Seasonal cycle of the limitation terms of *Trichodesmium* production in a) the South Pacific and b) the North Pacific. The right scale (in brown) represents the total limitation.

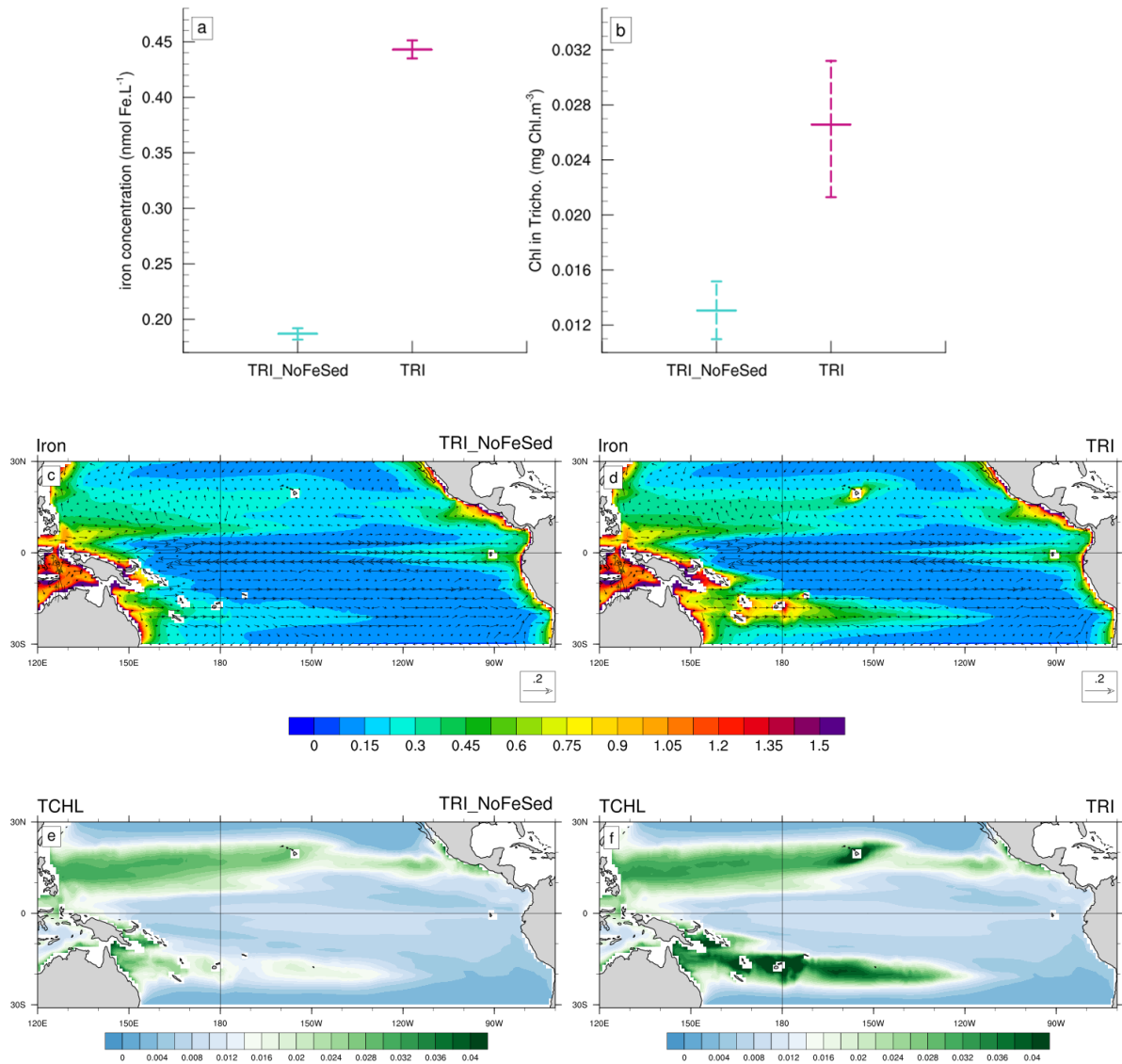


Figure 9. Top : Minimum, mean and maximum in the South box (Fig 1c) of (a) the iron concentrations (in nmol Fe.L⁻¹), and (b) of the chlorophyll concentrations of *Trichodesmium* (in mg Chl.m⁻³).

Bottom : Annual mean iron concentrations (shading ; in nmol Fe.L⁻¹) and current velocities (vectors ; in m.s⁻¹) for c) the TRI_NoFeSed simulation and d) the TRI simulation. Annual mean Chlorophyll concentrations of *Trichodesmium* (mg Chl.m⁻³) for e) the TRI_NoFeSed simulation and f) the TRI simulation. The concentrations have been averaged over the top 100m of the ocean. The current velocities are identical on the panels a and b.

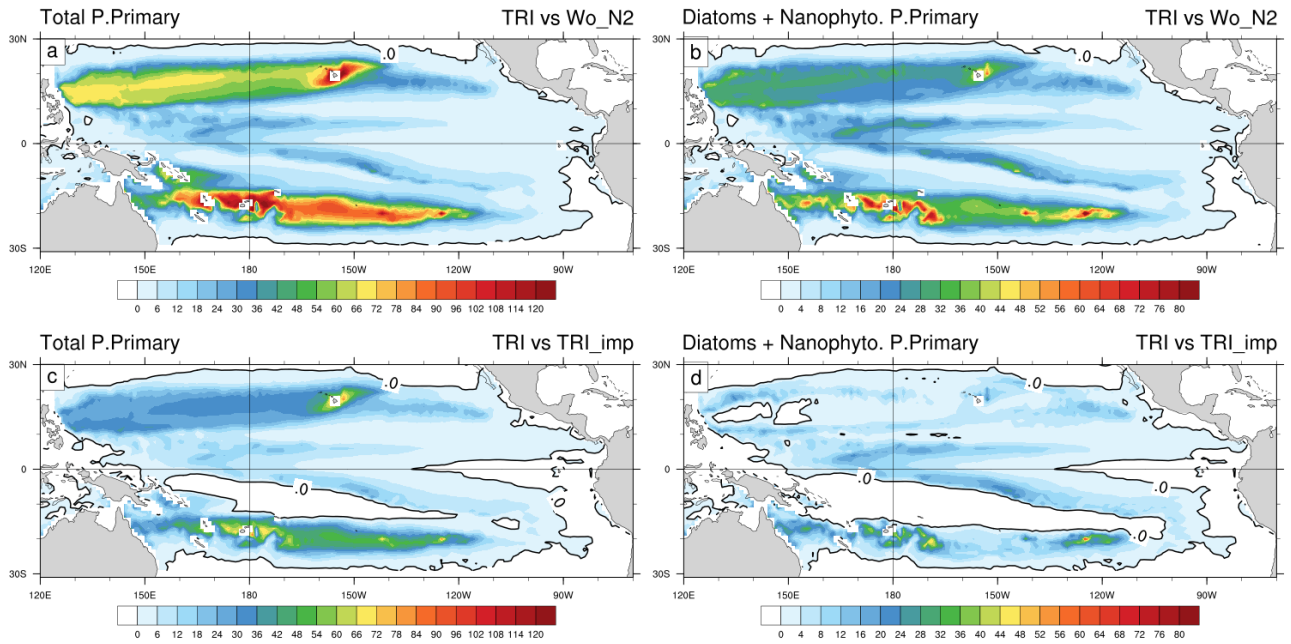


Figure 10. Percentage increase of primary production between the TRI simulation and the Wo_N2 simulation (top) and the TRI_imp simulation (bottom); The left panels show total primary production including the contribution of *Trichodesmium* whereas in the right panels, primary production only includes the contribution of diatoms and nanophytoplankton.

Table 1. Models parameters for Trichodemium and nanophytoplakton.

Parameters	Symbol	Unity	Value	Reference
Maximum growth rate for Tricho.	μ_{max}^{Tri}	d^{-1}	0.25	Breitbarth et al. (2007)
Maximum growth rate for Nano.	μ_{max}^{Nano}	d^{-1}	1.0	
Initial slope P-I Tricho.	αI	$(W.m^{-2})^{-1}.d^{-1}$	0.072	Breitbarth et al. (2008) and Hood et al. (2002)
Initial slope P-I Nano.	αI	$(W.m^{-2})^{-1}.d^{-1}$	2.0	
Microzoo preference for Tricho.	p_{Tri}^I	-	0.5	
Microzoo preference for Nano.	p_{Nano}^I	-	1.0	
Maximum Fe/C in Tricho.	$\theta_{max,Tri}^{Fe}$	$mol\ Fe.(mol\ C)^{-1}$	1.10^{-4}	Kustka et al. (2003)
Maximum Fe/C in Nano.	$\theta_{max,Nano}^{Fe}$	$mol\ Fe.(mol\ C)^{-1}$	4.10^{-5}	
Maintenance iron	m	$mol\ Fe.(mol\ C)^{-1}$	$1.4.10^{-5}$	Kustka et al. (2003)
Maintenance use efficiency	β	$mol\ C.(mol\ Fe)^{-1}.day^{-1}$	$1.4.10^{-4}$	Kustka et al. (2003)

Table 2. List and description of the different experiments.

Name configuration	N₂ fixation	Iron from sediment
TRI	explicit	yes
TRI_NoFeSed	explicit	no
TRI_imp	explicit	yes
Wo_N2	explicit	yes